




Macroscopic Wigner’s friend paradoxes: Consistency with weak macroscopic realismRia Rushin Joseph ^{1,2} Manushan Thenabadu,¹ Channa Hatharasinghe,¹ Jesse Fulton,¹
Run-Yan Teh,¹ P. D. Drummond,¹ and M. D. Reid ¹¹*Centre for Quantum Science and Technology Theory, Swinburne University of Technology, Melbourne 3122, Australia*²*School of Information Technology, Deakin University, Burwood Campus, Melbourne 3125, Australia* (Received 28 November 2022; revised 29 November 2023; accepted 17 January 2024; published 13 August 2024)

Wigner’s friend paradoxes highlight contradictions between measurements made by friends inside a laboratory and superobservers outside the laboratory, who have access to an entangled state of the measurement apparatus. Where there are two separated laboratories, the contradictions lead to no-go theorems for observer-independent facts, thus challenging concepts of objectivity. Here, we examine the paradoxes from the perspective of establishing consistency with macroscopic realism. We present versions of the Brukner-Wigner’s-friend and Frauchiger-Renner paradoxes in which the spin-1/2 systems measured by the friends correspond to two macroscopically distinct states. The local unitary operations U_{θ_j} that determine the measurement settings θ_j at each laboratory are carried out using nonlinear interactions, which are tailored to ensure that measurements need only distinguish between the macroscopically distinct states. The macroscopic paradoxes are perplexing, seemingly suggesting there is no objectivity in a macroscopic limit. However, we demonstrate consistency with a contextual weak form of macroscopic realism (wMR): The premise wMR asserts that each system j can be considered to have a definite spin outcome λ_{θ_j} , at the time after the system has undergone the local unitary rotation U_{θ_j} to prepare it in a suitable measurement basis. We further show that the paradoxical outcomes imply failure of deterministic macroscopic local realism and arise when there are unitary interactions U_{θ_j} occurring due to a change of measurement setting at both laboratories, with respect to the state prepared by each friend. In models which validate wMR, there is a breakdown of a subset of the assumptions that constitute the Bell-locality premise. A similar interpretation involving a contextual weak form of local realism exists for the original paradoxes.

DOI: [10.1103/PhysRevA.110.022219](https://doi.org/10.1103/PhysRevA.110.022219)**I. INTRODUCTION**

The Wigner’s friend paradox concerns a gedanken experiment in which inconsistencies arise between observations recorded by experimentalists either inside (the “friends”) or outside (the “superobservers”) the laboratory [1]. There is a distinction between systems that have undergone a “collapse” into an eigenstate due to measurement and systems which remain entangled with the laboratory apparatus. The inconsistencies can be quantified in the form of Brukner’s no-go theorem for “observer-independent facts,” whereby a record of the results of measurements exists in a way that can be viewed consistently between observers [2]. The no-go theorem applies to an extended Wigner’s friend paradox for two separated laboratories and adopts the locality assumption [3–7]. The inconsistencies have been further highlighted by the Frauchiger-Renner paradox [8]. As experiments support quantum predictions [9,10], the paradoxes challenge the concept of objectivity. This has motivated further work [9–24] including analyses involving consistent histories [15], Bohmian models [14], weak measurements [17], timeless formulations [21], and strong “local friendliness” no-go theorems [10].

In this paper, we present macroscopic versions of the extended Wigner’s friend and Frauchiger-Renner paradoxes in which *all* measurements leading to the inconsistent results are performed on a system “which has just two macroscopically distinguishable states available to it” [25–27]. This

includes the initial system measured by the friends in each laboratory, which is normally considered to be microscopic. The consequence is that one can apply, for each system and measurement, the definition of macroscopic realism put forward by Leggett and Garg [27,28]. Leggett and Garg’s macroscopic realism (MR) asserts that the system actually *be* in one or other state at any given time, meaning that the outcome of a measurement distinguishing between the two macroscopically distinct states has a predetermined value. We note that the definition of MR does not require knowledge about the “state” the system is in at a microscopic level.

With this definition, it might seem at first glance impossible to obtain consistency between macroscopic realism and the macroscopic Wigner’s friend paradoxes, which suggest there is no objectivity between observers for the outcomes of quantum measurements on a macroscopic spin. The paradoxes as applied to macroscopic qubits become especially puzzling, because apparently then there is no basis for objectivity even in a macroscopic limit.

In this paper, we examine the relationship of the paradoxes with macroscopic realism (MR), giving a resolution of the apparent inconsistencies. We consider two forms of MR, a deterministic form (dMR) which we show is negated by the paradoxes, and a weaker form (wMR), which we show is consistent with the quantum predictions and is similar to Bell’s idea of macroscopic “beables” [29]. The resolution is based on the dynamics of the unitary interaction

U_θ that determines the measurement setting for a spin measurement S_θ . In a contextual model of quantum mechanics, the state of the system after the interaction differs from that before the interaction. We demonstrate that the premise of MR if applied to the system at the time t_i *after* the dynamics $U_\theta(t)$ (when the measurement settings are fixed) is consistent with the quantum predictions: The premise of MR if applied to the system as it exists *prior* to the dynamics $U_\theta(t)$ is falsifiable by the quantum predictions. This leads to the two definitions of MR [30–33]. The first is a weaker (more minimal) assumption, referred to as *weak macroscopic realism* (wMR). The second definition is a stronger assumption that postulates predetermined variables prior to all stages of measurement, along the lines of classical mechanics, and is referred to as *deterministic macroscopic realism* (dMR).

We therefore put forward an analysis of the Wigner’s friend experiments that validates an objective macroscopic realism, in which there is a predetermined value $\lambda_{\theta,i}$ for the outcome of the measurement on the macroscopic two-state system defined at a time t_i , in accordance with wMR. The system is objectively in a state of definite qubit value $\lambda_{\theta,i}$, at the time t_i *once* the system has undergone the appropriate local unitary rotation U_θ to prepare it in the suitable basis, meaning that the records of the friend (who makes a measurement inside the laboratory) and the superobserver (who makes measurements on the entire laboratory) agree on such values. The paradoxical outcomes between the two types of observers (friends and superobservers) at different laboratories illustrate a failure of dMR, which we show manifests as a violation of a macroscopic Brukner-Bell-Wigner inequality in both the extended Wigner’s friend experiment, and the Frauchiger-Renner version.

We further show that the inconsistencies between the different observers arise where there are two nonzero unitary rotations, U_θ and U_ϕ , one at each of the two laboratories, giving a change of measurement setting of the superobservers with respect to the friends at *both* available laboratories. In this case, the assumption of locality is justified by deterministic MR but *not* by weak MR. The quantum predictions that violate Brukner-Bell-Wigner or Bell inequalities are therefore *not inconsistent with weak macroscopic realism* (wMR).

In fact, the premise of wMR implies only a *partial locality*, which asserts no-disturbance to the value of $\lambda_{\theta,i}$ for the state created at the time t_i , *after* the local unitary $U_\theta(t)$ has taken place. It is postulated that there can be no change to the value of $\lambda_{\theta,i}$ due to any further unitary interaction U_ϕ occurring at the other laboratory after the time t_i . The premise wMR does not imply locality in the full sense: It cannot be assumed that the outcome of a spin measurement S_θ at one laboratory A is not affected by an interaction U_ϕ occurring to fix the measurement setting ϕ at the other laboratory B *if* the local unitary interaction U_θ at A has not yet occurred. Here, we assume no relative motion between the laboratories and that all observers are in the laboratory frame.

The formulation of the macroscopic paradoxes is achieved by a direct mapping of the microscopic gedanken experiment onto a macroscopic one, the spin qubits $|\uparrow\rangle$ and $|\downarrow\rangle$ corresponding to two macroscopically distinct orthogonal states. We illustrate with two examples: two coherent states $|\alpha\rangle$ and $|\alpha\rangle$ where $\alpha \rightarrow \infty$, and two groups of N correlated spins.

The unitary operations U_θ required for the measurement of a spin component S_θ are realized by a Kerr Hamiltonian H_{NL} , where the value of θ is determined by the time of interaction with a nonlinear medium, or a sequence of CNOT gates.

The interpretation given in this paper motivates a similar interpretation for the original paradoxes, where the friends make microscopic spin measurements. In that interpretation, wMR is replaced by a weak version of local realism (wLR), which specifies a predetermined value $\lambda_{\theta,i}$ for the outcome of a measurement S_θ , for the system prepared at time t_i *after* the unitary interaction U_θ determining the choice of measurement setting θ has been carried out. The interaction U_θ prepares the system with respect to a measurement basis, in a state given as the superposition $|\uparrow\rangle_\theta + |\downarrow\rangle_\theta$ of eigenstates of the spin observable S_θ . In this contextual model, the state is only completely described once the measurement basis is specified. Similar contextual models have been given for Bell violations [30–34] and, in a full probabilistic formulation, for quantum measurement [35,36].

Overview of paper. The paper is organized as follows: In Sec. II, we summarize the Wigner’s friend and Frauchiger-Renner gedanken paradoxes. For our work involving macroscopic superposition states, it proves convenient to consider two strategies, one involving measurements of S_z and S_x as in the original examples, and the other involving measurements of S_z and S_y . We illustrate the fully macroscopic versions of the paradoxes in Sec. III, where we show a violation of the Brukner-Bell-Wigner inequality. In Sec. IV, we demonstrate the failure of deterministic macroscopic (local) realism (dMR) for both paradoxes. Weak macroscopic realism (wMR) is explained in Sec. V, where it is shown how wMR can be compatible with violations of the Brukner-Bell-Wigner and Clauser-Horne-Shimony-Holt (CHSH) Bell inequalities. We prove a sequence of results for wMR. In Sec. VI, the consistency of the paradoxes with wMR is illustrated by way of an explicit wMR model. This is done by comparing with the predictions of certain quantum mixtures that are valid from one or other of the friends’ perspectives. A conclusion is given in Sec. VII.

II. WIGNER’S FRIEND PARADOXES

A. Observer-independent facts no-go theorem: Brukner Bell-Wigner test

We first summarize the theorem introduced by Brukner for an extended version of the Wigner’s friend paradox [2]. A spin-1/2 system is in a closed laboratory L where Wigner’s friend F can make a measurement on a spin-1/2 system to measure the z component σ_z . This means that the spin system will become entangled with a second more macroscopic system that exists in the laboratory. (Ultimately, as each piece of apparatus becomes entangled, the macroscopic apparatus includes the friend.) From the friend’s perspective, after the measurement, the system has collapsed into a state that has a definite value for the spin σ_z measurement. To Wigner, who is outside the laboratory, the friend’s measurement is described by a unitary interaction, and the combined state of the spin and friend is given by

$$|\Phi\rangle_{SF} = \frac{1}{\sqrt{2}}(|\uparrow\rangle_z|F_{z+}\rangle + |\downarrow\rangle_z|F_{z-}\rangle). \quad (1)$$

Here, $|\uparrow\rangle_z$ and $|\downarrow\rangle_z$ are the eigenstates of σ_z . The $|F_{z+}\rangle$ and $|F_{z-}\rangle$ are states for the macroscopic measuring apparatus, which we might envisage to be a pointer on a measurement dial that indicates the result of the measurement to be either a positive outcome +1 (spin ‘‘up’’), or a negative outcome -1 (spin ‘‘down’’), respectively. We refer to Wigner’s possible spin measurement, which involves a more macroscopic state and need not be restricted to just one component, using the notation S_z , S_x , and S_y . Wigner’s description of the combined state is that of a superposition. Hence, the interpretation of the overall state of the laboratory is different, or unclear, since the superposition is not equivalent to the mixture of the two states $|\uparrow\rangle_z|F_{z+}\rangle$ and $|\uparrow\rangle_z|F_{z-}\rangle$.

A no-go theorem relating to the paradox was presented by Brukner, who established a theoretical framework in which one can account for observer-independent facts [2]. The notion of observer-independent facts is tested by carrying out a Bell-Wigner experiment. Based on the work of Brukner, a violation of a Bell-Wigner inequality implies a failure of the conjunction of: (1) locality, (2) free choice (freedom for all parties to choose their measurement settings), and (3) observer-independent facts (a record from a measurement should be a fact of the world that all observers can agree on). The difference between a Bell test and a Bell-Wigner test lies in the third assumption; a Bell-Wigner test assumes observer-independent facts, while a Bell test assumes hidden variables that describe (for maximally correlated Bell states) predetermined measurement outcomes. Locality is defined by Bell in the original derivation of Bell’s inequalities and implies no instantaneous influences between spacelike-separated systems.

Brukner considered a pair of superobservers (Alice and Bob) who can carry out experiments on two separate laboratories L_A and L_B that each consist of a spin-1/2 system and the superobservers’ friends, Charlie and Debbie, respectively (Fig. 1). Measurement settings A_1 and A_2 correspond to the observational statements of Charlie and Alice, while the measurement settings B_1 and B_2 correspond to the observational statements of Debbie and Bob. The conjunction of the assumptions leads to the Bell-Wigner inequality in the form of a Clauser-Horne-Shimony-Holt (CHSH) Bell inequality [4–7,29]

$$S = |\langle A_1 B_1 \rangle + \langle A_1 B_2 \rangle + \langle A_2 B_1 \rangle - \langle A_2 B_2 \rangle| \leq 2. \quad (2)$$

A violation would imply a contradiction with the assumptions.

It has been shown that the inequality can be violated [2]. For our analysis using cat states, it will prove convenient to consider two strategies, one involving measurements of spins S_z and S_x as in the original example, and the other involving measurements of spins S_z and S_y . We therefore propose that Charlie and Debbie receive an entangled state of spin-1/2 particles given as

$$\begin{aligned} |\psi_{\pm}\rangle &= -\sin\frac{\theta}{2}|\phi^{\mp}\rangle + \varepsilon_{\pm}\cos\frac{\theta}{2}|\psi^{\pm}\rangle \\ &= -\sin\frac{\theta}{2}(|\uparrow\rangle_{z,C}|\uparrow\rangle_{z,D} \mp |\downarrow\rangle_{z,C}|\downarrow\rangle_{z,D})/\sqrt{2} \\ &\quad + \varepsilon_{\pm}\cos\frac{\theta}{2}(|\uparrow\rangle_{z,C}|\downarrow\rangle_{z,D} + |\downarrow\rangle_{z,C}|\uparrow\rangle_{z,D})/\sqrt{2}, \end{aligned} \quad (3)$$

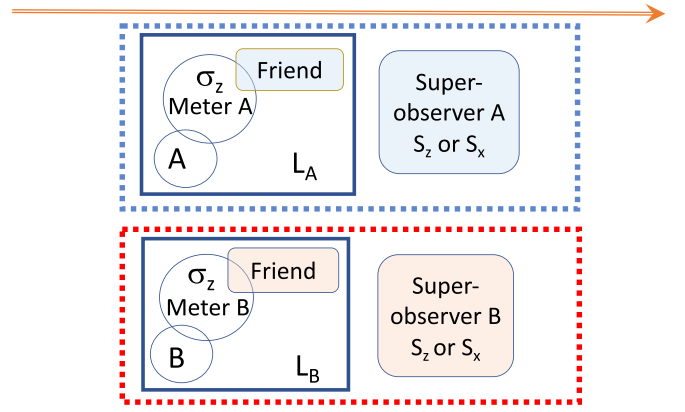


FIG. 1. Wigner’s friend paradox: The two entangled systems A and B are prepared and then separated into laboratories L_A and L_B . The friends in each laboratory measure the spin σ_z of the local system, using a macroscopic meter. The superobservers outside each laboratory can measure the local macroscopic spins S_z or S_x of the entire lab systems. In our analysis, we generalize to also consider where the superobservers measure S_z or S_y . The arrow depicts the direction of time, meaning that the superobservers make their measurements after those of the friends.

where $|\phi^{\mp}\rangle = \frac{1}{\sqrt{2}}(|\uparrow\rangle_{z,C}|\uparrow\rangle_{z,D} \mp |\downarrow\rangle_{z,C}|\downarrow\rangle_{z,D})$ and $|\psi^{\pm}\rangle = \frac{1}{\sqrt{2}}(|\uparrow\rangle_{z,C}|\downarrow\rangle_{z,D} + |\downarrow\rangle_{z,C}|\uparrow\rangle_{z,D})$, with $\varepsilon_+ = 1$ and $\varepsilon_- = i$. The states $|\uparrow\rangle_{z,C}$, $|\downarrow\rangle_{z,C}$, and $|\uparrow\rangle_{z,D}$, $|\downarrow\rangle_{z,D}$ denote the spin-1/2 eigenstates of S_z as prepared in Charlie and Debbie’s laboratory, respectively. We define two initial states $|\psi_+\rangle$ and $|\psi_-\rangle$, which will allow violation of the inequality (2) for the pair of measurements S_z and S_x , and the pair of measurements S_z and S_y , respectively.

Next, Charlie and Debbie each perform a measurement. After completing the coupling needed for their measurement on the system prepared in $|\psi_{\pm}\rangle$, the overall state becomes

$$|\tilde{\Psi}_{\pm}\rangle = -\sin\frac{\theta}{2}|\Phi^{\mp}\rangle + \varepsilon_{\pm}\cos\frac{\theta}{2}|\Psi^{\pm}\rangle, \quad (4)$$

where

$$\begin{aligned} |\Phi^{\mp}\rangle &= \frac{1}{\sqrt{2}}(|A_{up}\rangle|B_{up}\rangle \mp |A_{down}\rangle|B_{down}\rangle), \\ |\Psi^{\pm}\rangle &= \frac{1}{\sqrt{2}}(|A_{up}\rangle|B_{down}\rangle + |A_{down}\rangle|B_{up}\rangle), \end{aligned} \quad (5)$$

with $|A_{up}\rangle = |\uparrow\rangle_{z,C}|C_{z+}\rangle_C$, $|A_{down}\rangle = |\downarrow\rangle_{z,C}|C_{z-}\rangle_C$, $|B_{up}\rangle = |\uparrow\rangle_{z,D}|D_{z+}\rangle_D$, and $|B_{down}\rangle = |\downarrow\rangle_{z,D}|D_{z-}\rangle_D$. Here, $|C_{z\pm}\rangle_C$ and $|D_{z\pm}\rangle_D$ are the states of the macroscopic measurement apparatus (the friends) in the respective laboratories.

For the choice of initial state $|\psi_+\rangle$, we consider the measurement settings

$$\begin{aligned} A_1 &\equiv A_z = |A_{up}\rangle\langle A_{up}| - |A_{down}\rangle\langle A_{down}|, \\ A_2 &\equiv A_x = |A_{up}\rangle\langle A_{down}| + |A_{down}\rangle\langle A_{up}|, \end{aligned} \quad (6)$$

corresponding to macroscopic spin z and spin x measurements in Charlie’s laboratory, and

$$\begin{aligned} B_1 &\equiv B_z = |B_{up}\rangle\langle B_{up}| - |B_{down}\rangle\langle B_{down}|, \\ B_2 &\equiv B_x = |B_{up}\rangle\langle B_{down}| + |B_{down}\rangle\langle B_{up}|, \end{aligned} \quad (7)$$

corresponding to macroscopic spin z and spin x measurements in Debbie's laboratory. The Bell-Wigner CHSH inequality for this case is

$$S = |\langle A_z B_z \rangle + \langle A_z B_x \rangle + \langle A_x B_z \rangle - \langle A_x B_x \rangle| \leq 2. \quad (8)$$

It has been shown that this inequality is violated for $\theta = \pi/4$ with $S = -2\sqrt{2}$.

On the other hand, for the choice of initial state $|\psi_-\rangle$, we consider the measurement settings

$$\begin{aligned} A_1 &\equiv A_z = |A_{up}\rangle\langle A_{up}| - |A_{down}\rangle\langle A_{down}|, \\ A_2 &\equiv A_y = (|A_{up}\rangle\langle A_{down}| - |A_{down}\rangle\langle A_{up}|)/i, \end{aligned} \quad (9)$$

corresponding to macroscopic spin z and spin y measurements in Charlie's laboratory, and

$$\begin{aligned} B_1 &\equiv B_z = |B_{up}\rangle\langle B_{up}| - |B_{down}\rangle\langle B_{down}|, \\ B_2 &\equiv B_y = (|B_{up}\rangle\langle B_{down}| - |B_{down}\rangle\langle B_{up}|)/i, \end{aligned} \quad (10)$$

corresponding to macroscopic spin z and spin y measurements in Debbie's laboratory. The Bell-Wigner CHSH inequality for this case is

$$S = \langle A_z B_z \rangle + \langle A_z B_y \rangle + \langle A_y B_z \rangle - \langle A_y B_y \rangle \leq 2. \quad (11)$$

This is the case of interest in this paper. We evaluate the correlations as follows: Directly, we find

$$\langle A_z B_z \rangle = -\cos \theta.$$

To evaluate $\langle A_z B_y \rangle$, we write the state in the new basis, by noting the standard transformation

$$\begin{aligned} |\uparrow\rangle_y &= \frac{1}{\sqrt{2}}(|\uparrow\rangle_z + i|\downarrow\rangle_z), \\ |\downarrow\rangle_y &= \frac{1}{\sqrt{2}}(|\uparrow\rangle_z - i|\downarrow\rangle_z), \end{aligned} \quad (12)$$

where $|\uparrow\rangle_y$ and $|\downarrow\rangle_y$ are the eigenstates of the Pauli spin σ_y , with eigenvalues $+1$ and -1 , respectively. Hence, we write $|\uparrow\rangle_z = (|\uparrow\rangle_y + |\downarrow\rangle_y)/\sqrt{2}$ and $|\downarrow\rangle_z = -i(|\uparrow\rangle_y - |\downarrow\rangle_y)/\sqrt{2}$. Substituting, we find

$$\begin{aligned} \langle A_z B_y \rangle &= \langle A_y B_z \rangle = -\sin \theta, \\ \langle A_y B_y \rangle &= \cos \theta. \end{aligned}$$

The Bell-Wigner inequality is violated with $|S| = 2\sqrt{2}$ for $\theta = \pi/4$. An experimental test supporting the predictions of quantum mechanics has been carried out by Proietti *et al.* [9].

B. Frauchiger-Renner paradox

Here we outline the Frauchiger-Renner paradox [8] which also examines the Wigner friend's thought experiment, arriving at a contradiction between the friends inside the laboratories and the observers outside. We follow the summary given by Losada *et al.* [15].

First, a biased quantum coin tossed by the friend F_A in laboratory A gives outcomes h and t with probabilities $1/3$ and $2/3$, respectively. If the outcome is h or t , the friend F_B in the second laboratory L_B creates the spin-1/2 state $|\downarrow\rangle$ or $|\rightarrow\rangle = \frac{1}{\sqrt{2}}(|\uparrow\rangle + |\downarrow\rangle)$, respectively. Here, $|\hbar\rangle_z$, $|t\rangle_z$, and $|\uparrow\rangle_z$, $|\downarrow\rangle_z$ are the eigenstates of the Pauli spin observables σ_z^A and σ_z^B for two spin-1/2 systems at the spatially separated laboratories L_A and L_B , respectively.

In fact, the friend F_A has measured the state of the coin, by first coupling with a device in L_A , later measured by the friend. The macroscopic states $|H\rangle_z$ and $|T\rangle_z$ ultimately represent all macroscopic devices leading to the measurement outcome. The $|H\rangle_z$ and $|T\rangle_z$ are the macroscopic states of the laboratory L_A giving the measurement outcomes h and t respectively, being eigenstates of the observable denoted S_z^A . The coupling to the second laboratory L_B is described by an interaction Hamiltonian. The laboratory L_A is coupled to L_B so that a final entangled state

$$|\psi_{zz}\rangle_{FR} = \frac{1}{\sqrt{3}}|H\rangle_z|\downarrow\rangle_z + \sqrt{\frac{2}{3}}|T\rangle_z|\rightarrow\rangle_z \quad (13)$$

is created. Here, $|\rightarrow\rangle_z = \frac{1}{\sqrt{2}}(|\uparrow\rangle_z + |\downarrow\rangle_z)$, where $|\uparrow\rangle_z$ and $|\downarrow\rangle_z$ are the macroscopic states of L_B giving the "up" and "down" outcomes respectively for the observable denoted S_z^B .

The second step is that the external superobservers W_A and W_B make measurements of S_x on the systems in L_A and L_B , respectively. These observables are defined so that the eigenstates of S_x^A for laboratory L_A are

$$\begin{aligned} |H\rangle_x &= \frac{1}{\sqrt{2}}|H\rangle_z + \frac{1}{\sqrt{2}}|T\rangle_z, \\ |T\rangle_x &= \frac{1}{\sqrt{2}}|H\rangle_z - \frac{1}{\sqrt{2}}|T\rangle_z. \end{aligned} \quad (14)$$

Similarly, the "up" and "down" eigenstates of S_x^B for laboratory L_B are

$$\begin{aligned} |\uparrow\rangle_x &= \frac{1}{\sqrt{2}}|\uparrow\rangle_z + \frac{1}{\sqrt{2}}|\downarrow\rangle_z, \\ |\downarrow\rangle_x &= \frac{1}{\sqrt{2}}|\uparrow\rangle_z - \frac{1}{\sqrt{2}}|\downarrow\rangle_z. \end{aligned} \quad (15)$$

We first consider where W_A and W_B both measure S_x . We rewrite the state (13) in terms of the different bases. In the new basis, we find

$$\begin{aligned} |\psi_{xx}\rangle_{FR} &= \frac{\sqrt{3}}{2}|H\rangle_x|\uparrow\rangle_x - \frac{1}{\sqrt{12}}|T\rangle_x|\uparrow\rangle_x \\ &\quad - \frac{1}{\sqrt{12}}|H\rangle_x|\downarrow\rangle_x - \frac{1}{\sqrt{12}}|T\rangle_x|\downarrow\rangle_x. \end{aligned} \quad (16)$$

From the above expression, we see that the probability is $1/12$ for obtaining outcomes T and \downarrow .

But now, if the friend F_B had measured σ_z , and W_A measures S_x^A , we would write

$$|\psi_{xz}\rangle_{FR} = \frac{1}{\sqrt{6}}|H\rangle_x|\uparrow\rangle_z - \frac{1}{\sqrt{6}}|T\rangle_x|\uparrow\rangle_z + \frac{2}{\sqrt{6}}|H\rangle_x|\downarrow\rangle_z. \quad (17)$$

Here, the probability for $|T\rangle_x|\downarrow\rangle_z$ is zero. This implies that, when W_A obtains T for S_x , it is confirmed with certainty that F_B would have obtained \uparrow for the measurement of σ_z , which in turn would imply for friend F_B that F_A had obtained t for σ_z , (since the \uparrow state for σ_z at system B is only created when F_A would have obtained t for σ_z). In the basis of σ_z for L_A and S_x for L_B , we would write

$$|\psi_{zx}\rangle_{FR} = \frac{1}{\sqrt{6}}|H\rangle_z(|\uparrow\rangle_x - |\downarrow\rangle_x) + \sqrt{\frac{2}{3}}|T\rangle_z|\uparrow\rangle_x. \quad (18)$$

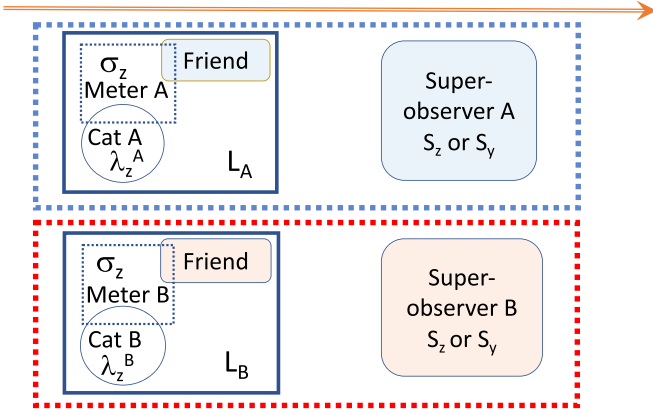


FIG. 2. A macroscopic paradox with cat states: The two entangled systems A and B are prepared and then separated into laboratories L_A and L_B , as in Fig. 1. Here, the systems A and B are themselves macroscopic, meaning that the spins values $+1$ and -1 for σ_z correspond to macroscopically distinct states of the system. The premise of macroscopic realism asserts that the value of the spin outcome σ_z is predetermined, given by a variable λ_z .

As the outcome t for σ_z is perfectly correlated with the state $|\uparrow\rangle_x$, it is certain from (18) that W_B would then get \uparrow for their measurement S_x in laboratory L_B . But (16) gives a nonzero probability for W_A and W_B getting T and \downarrow for S_x , and this is the basis of the Frauchiger-Renner (FR) paradox.

III. WIGNER'S FRIEND PARADOXES USING CAT STATES

In this section, we present the paradox in terms of cat states [25,26], where the *original* spin-1/2 system measured by the friends is a macroscopic one, and the two spin-1/2 eigenstates are macroscopically distinct states (macroscopic qubits). This is depicted in Fig. 2.

A. Two stages of the spin measurement

An important aspect of the Wigner's friend paradox is that the measurement of spin occurs in two stages, one of which is reversible. In the cat example, this is also true. We examine a specific macroscopic realization, in order to analyze the dynamics of the measurements.

The first reversible stage of the spin measurement is the unitary interaction U_θ which determines the measurement setting, i.e., the component of spin that will be measured, whether σ_z , σ_x , or σ_y . This stage transforms an initial eigenstate into a superposition of two eigenstates: e.g., $|\uparrow\rangle \rightarrow \frac{1}{\sqrt{2}}(|\uparrow\rangle + |\downarrow\rangle)$. In a photonic Bell experiment, the unitary transformations are achieved by polarizing beam splitters (PBS). The unitary transformations U_θ for coherent-state qubits are explained below.

The second stage of measurement occurs after the unitary rotation U_θ . Once the unitary rotation has been performed, the measurement setting has been selected, and the system is prepared for a final stage of measurement, that we refer to as the “pointer” measurement. This would usually include a final amplification and detection stage, involving a coupling to a meter, and a read-out to a second system, i.e., an observer. We might also refer to this stage of measurement as the “collapse”

stage because, from the perspective of the observer making the measurement, this stage is irreversible.

B. Macroscopic spins

The paradoxes involve spin measurements on each of two separated systems, labeled A and B (Fig. 2). For macroscopic qubits, the spin measurements are defined by two macroscopically distinct states. For example, the macroscopic two-state systems of the entire labs at B and A are denoted by $|\uparrow\rangle$ and $|\downarrow\rangle$, and $|H\rangle$ and $|T\rangle$, respectively. The corresponding two-state spin observables are

$$\begin{aligned} S_z^A &= |H\rangle\langle H| - |T\rangle\langle T|, \\ S_x^A &= |H\rangle\langle T| + |T\rangle\langle H|, \\ S_y^A &= \{|H\rangle\langle T| - |T\rangle\langle H|\}/i, \end{aligned} \quad (19)$$

and

$$\begin{aligned} S_z^B &= |\uparrow\rangle\langle\uparrow| - |\downarrow\rangle\langle\downarrow|, \\ S_x^B &= |\uparrow\rangle\langle\downarrow| + |\downarrow\rangle\langle\uparrow|, \\ S_y^B &= \{|\uparrow\rangle\langle\downarrow| - |\downarrow\rangle\langle\uparrow|\}/i. \end{aligned} \quad (20)$$

The paradoxes involve noncommuting spin measurements. We therefore will seek a unitary transformation U_x^{-1} that transforms the eigenstates of S_z into eigenstates of S_x :

$$\begin{aligned} |H\rangle &\rightarrow (|H\rangle + |T\rangle)/\sqrt{2}, \\ |T\rangle &\rightarrow (|H\rangle - |T\rangle)/\sqrt{2}, \end{aligned} \quad (21)$$

or else the transformation U_y^{-1} that transforms the eigenstates of S_z into eigenstates of S_y :

$$\begin{aligned} |H\rangle &\rightarrow (|H\rangle + i|T\rangle)/\sqrt{2}, \\ |T\rangle &\rightarrow (|H\rangle - i|T\rangle)/\sqrt{2} \end{aligned} \quad (22)$$

(and similarly for $|\uparrow\rangle$ and $|\downarrow\rangle$).

In a macroscopic Wigner-friend paradox, the *initial* spin-1/2 system measured by the friend is based on two macroscopically distinct states. We propose three sorts of macroscopic (or mesoscopic) qubits. The first two are presented in Appendix A 1. For the third, the spins $|\uparrow\rangle$ and $|\downarrow\rangle$ are the macroscopically distinct coherent states $|\alpha\rangle$ and $|\alpha\rangle$, defined for a field mode, where α is large and real (Fig. 2). In the limit $\alpha \rightarrow \infty$, the two states are orthogonal, and one defines two-state spin observables, for lab A , as

$$\begin{aligned} \sigma_z^A &= |\alpha\rangle\langle\alpha| - |\alpha\rangle\langle\alpha|, \\ \sigma_x^A &= |\alpha\rangle\langle\alpha| + |\alpha\rangle\langle\alpha|, \\ \sigma_y^A &= \{|\alpha\rangle\langle\alpha| - |\alpha\rangle\langle\alpha|\}/i. \end{aligned} \quad (23)$$

There is a direct mapping between the qubits $|\uparrow\rangle$ and $|\downarrow\rangle$ and the macroscopic qubits $|\alpha\rangle$ and $|\alpha\rangle$. Similarly,

$$\begin{aligned} \sigma_z^B &= |\beta\rangle\langle\beta| - |\beta\rangle\langle\beta|, \\ \sigma_x^B &= |\beta\rangle\langle\beta| + |\beta\rangle\langle\beta|, \\ \sigma_y^B &= \{|\beta\rangle\langle\beta| - |\beta\rangle\langle\beta|\}/i, \end{aligned} \quad (24)$$

where $|\beta\rangle$ and $|\beta\rangle$ (β is large and real) are macroscopically distinct coherent states for lab B . We consider quadrature

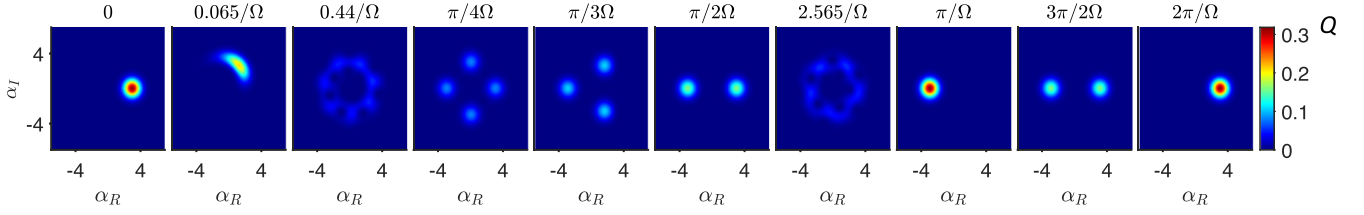


FIG. 3. The time sequence as the system A prepared at time $t = 0$ in a coherent state $|\alpha\rangle$ evolves according to H_{NL}^A of Eq. (26). This evolution is used to perform the rotation of basis necessary to carry out the spin measurement σ_y^A . The time of evolution is given above each snapshot. The cat state [Eq. (27)] given by $U_{\pi/4}^A|\alpha\rangle \equiv U_A(\pi/2\Omega)|\alpha\rangle$ is formed at time $t = \pi/2\Omega$. The contour graphs show surface plots of the Q function $Q(\alpha_0)$ with $\alpha = 4$ (refer Sec. VI for definitions). At the times $t = \pi/2\Omega$ and $3\pi/2\Omega$, the state of the system is expressible as a superposition of the coherent states $|\alpha\rangle$ and $|\alpha\rangle$. Here, α_r and α_i are the real and imaginary components of α_0 . The evolution is periodic with period $2\pi/\Omega$ and hence $(U_{\pi/4}^A)^{-1} = U_A(3\pi/2\Omega)$.

phase amplitude observables

$$\begin{aligned}\hat{X}_A &= (\hat{a} + \hat{a}^\dagger)/2, \\ \hat{P}_A &= (\hat{a} - \hat{a}^\dagger)/2i,\end{aligned}\quad (25)$$

defined for the field mode of lab A , where \hat{a} is the field annihilation operator [37]. The two states $|\alpha\rangle$ and $|\alpha\rangle$ can be distinguished by a measurement of \hat{X}_A . The sign of the outcome gives the qubit value, whether $+1$ or -1 . The measurement \hat{X}_A constitutes the *pointer measurement* of the system. Similar observables \hat{X}_B and \hat{P}_B are defined for lab B , the boson annihilation operator for the field at B being denoted by \hat{b} .

C. Measuring the different spin components

We next consider how to realize the first stage of the measurement, which determines the measurement setting, i.e., whether σ_z , σ_y , or σ_x will be measured. For the spins defined by the coherent states, the unitary transformation for U_y^A can be achieved using a Kerr nonlinearity, modeled by the Hamiltonian [38]

$$H_{NL}^A = \hbar\Omega\hat{n}_A^2, \quad (26)$$

where $\hat{n}_A = \hat{a}^\dagger\hat{a}$ is the number operator. After an interaction time $t = \pi/2\Omega$, the field of lab A initially prepared in a coherent state $|\alpha\rangle$ becomes a cat state. We find [37]

$$U_A\left(\frac{\pi}{2\Omega}\right)|\alpha\rangle = \frac{e^{-i\pi/4}}{\sqrt{2}}(|\alpha\rangle + i|\alpha\rangle), \quad (27)$$

where $U_A(t) = e^{-iH_{NL}^A t/\hbar}$. The dynamics is plotted in Fig. 3, where contour plots of the Q function [39] are presented after various times of evolution. We use the notation $U_A \equiv U_{\pi/4}^A \equiv U_A(\pi/2\Omega)$ to denote the transformation. Hence, for (22), we select $U_y = U_A^{-1} = (U_{\pi/4}^A)^{-1}$. The realization of the inverse of U_A^{-1} is achieved by evolving for a time $3\pi/2\Omega$. Here, we consider a system A in the lab A , but a similar interaction H_{NL}^B can be performed on a system B in lab B . Here, $H_{NL}^B = \hbar\Omega\hat{n}_B^2$ where $\hat{n}_B = \hat{b}^\dagger\hat{b}$.

Hence, the unitary interactions associated with the measurements S_y for each system are performed via the inverse of $U_{\pi/4}^A$ and $U_{\pi/4}^B$. Thus, we write

$$\begin{aligned}|\pm\rangle_{y,A} &= U_{\pi/4}^A|\pm\alpha\rangle_z = \frac{e^{-i\pi/4}}{\sqrt{2}}(|\pm\alpha\rangle_z + i|\mp\alpha\rangle_z), \\ |\pm\rangle_{y,B} &= U_{\pi/4}^B|\pm\beta\rangle_z = \frac{e^{-i\pi/4}}{\sqrt{2}}(|\pm\beta\rangle_z + i|\mp\beta\rangle_z),\end{aligned}\quad (28)$$

where we use that $U_A(t) = e^{-iH_{NL}^A t/\hbar}$ and $U_B(t) = e^{-iH_{NL}^B t/\hbar}$ as in (27). The different overall phase compared with the definition (22) does not change that the states are eigenstates of σ_y . This gives the required transformation, on denoting $|\pm\rangle_{z,A} \equiv |\pm\alpha\rangle_z$ and $|\pm\rangle_{y,A} \equiv |\pm\alpha\rangle_{y,A}$. It is straightforward to verify that $|\pm\rangle_{y,A}$ are the eigenstates of σ_y^A , given by Eq. (23), where $\alpha \rightarrow \infty$.

To rewrite the basis states for z in the basis for y , we operate on the states by $U_A^{-1}(U_B^{-1})$:

$$\begin{aligned}|\pm\alpha\rangle_z &= U_A^{-1}|\pm\alpha\rangle_y \\ &= \frac{e^{i\pi/4}}{\sqrt{2}}(|\pm\alpha\rangle_y - i|\mp\alpha\rangle_y).\end{aligned}\quad (29)$$

More generally, for a state $|\psi\rangle$ written as a superposition of the eigenstates of σ_z the transformation into the eigenstates of σ_y is given by

$$U_y|\psi\rangle \equiv U_A^{-1}|\psi\rangle. \quad (30)$$

A similar local transformation takes place on system B .

In summary, the system A can be prepared at time $t = 0$ in a superposition of the eigenstates of σ_z ,

$$|\psi\rangle = a|\alpha\rangle + b|\alpha\rangle, \quad (31)$$

where a and b are probability amplitudes. The measurement of $\hat{\sigma}_z$ is carried out by a direct measurement of the quadrature \hat{X}_A to determine the sign of \hat{X}_A , since α is real. To measure $\hat{\sigma}_y$, a rotation of basis is first necessary. We need to “rewrite” the state $|\psi\rangle$ as a superposition of the basis states of σ_y . This is achieved by the unitary operation $U_y = U_A^{-1}$. Thus the system evolves as

$$\begin{aligned}U_y|\psi\rangle &= aU_y|\alpha\rangle + bU_y|\alpha\rangle \\ &= \frac{e^{i\pi/4}}{\sqrt{2}}(c|\alpha\rangle + d|\alpha\rangle),\end{aligned}\quad (32)$$

where $c = a - ib$ and $d = -i(a + ib)$. This is equivalent to implementing eigenstates $|\uparrow\rangle_y = \frac{e^{-i\pi/4}}{\sqrt{2}}(|\uparrow\rangle_z + i|\downarrow\rangle_z)$ and $|\downarrow\rangle_y = \frac{ie^{-i\pi/4}}{\sqrt{2}}(|\uparrow\rangle_z - i|\downarrow\rangle_z) = \frac{e^{-i\pi/4}}{\sqrt{2}}(i|\uparrow\rangle_z + |\downarrow\rangle_z)$, which hence imply that $|\uparrow\rangle_z = \frac{e^{i\pi/4}}{\sqrt{2}}(|\uparrow\rangle_y - i|\downarrow\rangle_y)$ and $|\downarrow\rangle_z = \frac{e^{i\pi/4}}{\sqrt{2}}(-i|\uparrow\rangle_y + |\downarrow\rangle_y)$. Note, if we use the standard eigenstates $|\uparrow\rangle_y = \frac{1}{\sqrt{2}}(|\uparrow\rangle_z + i|\downarrow\rangle_z)$ and $|\downarrow\rangle_y = \frac{1}{\sqrt{2}}(|\uparrow\rangle_z - i|\downarrow\rangle_z)$, and then transform $|\psi\rangle = a|\uparrow\rangle_z + b|\downarrow\rangle_z$, we find $c = a - ib$ and $d = a + ib$, which gives the same probabilities of detection. We see that the outcome for spin σ_y is hence

given by the final pointer measurement, realized as the measurement of the (sign of the) quadrature \hat{X}_A for the system in the state (32) after rotation U_Y has been performed. Similar transformations and measurements can be performed on system B .

The cat states (27) have been created for a microwave field, using a dispersive Kerr interaction H_{NL}^A [40,41]. Similar effects are observed in Bose-Einstein condensates [42,43]. Other cat states have been created experimentally, using Rydberg atoms and CNOT gates [44–47]. In particular, the odd and even cat states $\approx|\alpha\rangle \pm |-\alpha\rangle$ which would allow the transformation U_x have been created in the laboratory [48]. Mechanisms for generation of such cat states are often limited to smaller systems, or else involve conditional measurements and/or optical, superconducting or optomechanical systems where dissipation plays a role [49–53]. In this paper, we focus on the cat states (27) generated by the simple unitary transformation U_y^A which is realizable using H_{NL}^A . The coherent-state qubits and unitary interactions U_y also allow macroscopic Bell violations [30,33,38], tests of macrorealism [30,33,54], macroscopic Bohm-Einstein-Podolsky-Rosen and GHZ paradoxes [31], and tests of two-dimensional macroscopic retrocausal models in delayed-choice Wheeler-Chaves-Lemos-Pienaar experiments [32].

D. Bell-Wigner tests with cat states

We now propose that the Bell-Wigner test given in Sec. II A be implemented with the spins $|\uparrow\rangle_{z,C}$ and $|\downarrow\rangle_{z,C}$ realized as the macroscopic coherent states $|\alpha\rangle_{z,C}$ and $|-\alpha\rangle_{z,C}$, and the spins $|\uparrow\rangle_{z,D}$ and $|\downarrow\rangle_{z,D}$ realized as the macroscopic states $|\alpha\rangle_{z,D}$ and $|-\alpha\rangle_{z,D}$, for large α . We explicitly write the state $|\psi_{-}\rangle$ given by Eq. (3) as

$$|\psi_{zz}\rangle_{WF} = A_{zz}(|\alpha\rangle_{z,C}|\alpha\rangle_{z,D} + |-\alpha\rangle_{z,C}|-\alpha\rangle_{z,D}) + B_{zz}(|\alpha\rangle_{z,C}|-\alpha\rangle_{z,D} + |-\alpha\rangle_{z,C}|\alpha\rangle_{z,D}), \quad (33)$$

where $A_{zz} = -\frac{1}{\sqrt{2}}\sin\theta/2$ and $B_{zz} = \frac{i}{\sqrt{2}}\cos\theta/2$. This state describes the systems when prepared in the z basis at both sites (labs). A method for experimentally mapping the state (3) onto the coherent-state version (33) is presented in Refs. [55,56].

The friends, Charlie and Debbie, then each perform a measurement of spin σ_z inside the labs. This involves coupling each system with a meter via interactions H_{Am} and H_{Bm} at the respective labs, and then further couplings to the friends in each laboratory. The overall interactions of the systems with the macroscopic apparatus are described by H_{AmF} and H_{BmF} . After the couplings, the overall state of the labs becomes $|\tilde{\Psi}_{-}\rangle = -\sin\frac{\theta}{2}|\Phi^{+}\rangle + i\cos\frac{\theta}{2}|\Psi^{+}\rangle$, where $|\Phi^{+}\rangle$ and $|\Psi^{+}\rangle$ are given by Eq. (5), with $|A_{up}\rangle = |\alpha\rangle_{z,C}|C_{z+}\rangle_C$, $|A_{down}\rangle = |-\alpha\rangle_{z,C}|C_{z-}\rangle_C$, $|B_{up}\rangle = |\alpha\rangle_{z,D}|D_{z+}\rangle_D$, and $|B_{down}\rangle = |-\alpha\rangle_{z,D}|D_{z-}\rangle_D$. Here, $|C_{z\pm}\rangle_C$ and $|D_{z\pm}\rangle_D$ are the states of the macroscopic measurement apparatus (the friends) in the respective labs. An example of the measurement interaction H_{Am} is given in the Appendix. With α real, the measurements of the quadrature phase amplitudes \hat{X}_A and \hat{X}_B [Eq. (25)] in the respective laboratories L_A and L_B will distinguish between the spin eigenstates in the limit of large α .

At each lab, the superobservers have the choice to measure either S_z or S_y (Fig. 2). To measure S_y , they can first

disentangle the system from the respective meter (by reversing H_{AmF} or H_{BmF}), and then perform the unitary evolution U_A^{-1} (or U_B^{-1}) as in (29), in order to change the measurement basis. A second stage of measurement (the pointer measurement) is then needed to give the final readout for S_y , meaning that the evolved system after U_A^{-1} (or U_B^{-1}) is then coupled to the meters and measurement apparatus, so that $|\alpha\rangle_{z,C} \rightarrow |\alpha\rangle_{z,C}|C_{z+}\rangle_C$ and $|-\alpha\rangle_{z,C} \rightarrow |-\alpha\rangle_{z,C}|C_{z-}\rangle_C$ (and $|\beta\rangle_{z,D} \rightarrow |\beta\rangle_{z,D}|D_{z+}\rangle_D$ and $|-\beta\rangle_{z,D} \rightarrow |-\beta\rangle_{z,D}|D_{z-}\rangle_D$). This amounts to a measurement of the quadrature phase amplitude \hat{X}_A (or \hat{X}_B) after the unitary operation U_A^{-1} (or U_B^{-1}). To instead measure S_z , there is no need to perform a subsequent unitary operation, because the system given by (33) is already prepared with respect to the measurement basis for spin z .

Consider measurements of S_z^A and S_y^B . After performing the necessary unitary rotations (including reversals), the system is given by

$$|\psi_{zy}\rangle_{WF} = A_{zy}(|\alpha\rangle_{z,C}|\alpha\rangle_{y,D} + i|-\alpha\rangle_{z,C}|-\alpha\rangle_{y,D}) + B_{zy}(|-\alpha\rangle_{z,C}|-\alpha\rangle_{y,D} + i|-\alpha\rangle_{z,C}|\alpha\rangle_{y,D}), \quad (34)$$

where $|\psi_{zy}\rangle_{WF} = U_B^{-1}|\psi_{zz}\rangle_{WF}$, $A_{zy} = \frac{1}{2}(-\sin\theta/2 + \cos\theta/2)$, and $B_{zy} = \frac{1}{2}(\sin\theta/2 + \cos\theta/2)$. Similarly, the state of the system prepared for pointer measurements S_y^A and S_z^B is

$$|\psi_{yz}\rangle_{WF} = A_{yz}(|\alpha\rangle_{y,C}|\alpha\rangle_{z,D} + i|-\alpha\rangle_{y,C}|-\alpha\rangle_{z,D}) + B_{yz}(i|\alpha\rangle_{y,C}|-\alpha\rangle_{z,D} - |-\alpha\rangle_{y,C}|\alpha\rangle_{z,D}) \quad (35)$$

where $|\psi_{yz}\rangle_{WF} = U_A^{-1}|\psi_{zz}\rangle_{WF}$, $A_{yz} = \frac{1}{2}(-\sin\theta/2 + \cos\theta/2)$, and $B_{yz} = \frac{1}{2}(\sin\theta/2 + \cos\theta/2)$. Similarly, for the measurements S_y^A and S_y^B ,

$$|\psi_{yy}\rangle_{WF} = A_{yy}(|\alpha\rangle_{y,C}|\alpha\rangle_{y,D} - |-\alpha\rangle_{y,C}|-\alpha\rangle_{y,D}) + B_{yy}(|\alpha\rangle_{y,C}|-\alpha\rangle_{y,D} + |-\alpha\rangle_{y,C}|\alpha\rangle_{y,D}), \quad (36)$$

where $|\psi_{yy}\rangle_{WF} = U_A^{-1}U_B^{-1}|\psi_{zz}\rangle_{WF}$, $B_{yy} = -\frac{1}{\sqrt{2}}\sin\theta/2$, and $A_{yy} = \frac{1}{\sqrt{2}}\cos\theta/2$. Comparing with Sec. II A, this gives an analogous violation of the Bell-Wigner inequality (11), with $S = 2\sqrt{2}$.

E. Frauchiger-Renner paradox using cat states

We now consider a test of the Frauchiger-Renner (FR) paradox based on cat states. The version of the FR paradox given in Sec. II C considers the option that the observers measure either spin z or spin x . We suppose instead that the observers at A and B measure either spin z or spin y , so that we may use the transformation (27). To do this, we consider that the state initially prepared between the laboratories is

$$|\psi_{zz}\rangle_{FR} = \frac{1}{\sqrt{3}}|H\rangle_{z,A}|\downarrow\rangle_{z,B} + \frac{1}{\sqrt{3}}|T\rangle_{z,A}(|\uparrow\rangle_{z,B} + i|\downarrow\rangle_{z,B}). \quad (37)$$

We suppose the state is prepared with respect to the basis S_z at each location, A and B . A paradox can be constructed as explained in Sec. II B above, but where the measurements of spin x are substituted as measurements of spin y .

We now present a version of the paradox using coherent states. We suppose the initial state created between the two

laboratories is

$$|\psi_{zz}\rangle_{FR} = \frac{1}{\sqrt{3}}|\alpha\rangle_z|-\beta\rangle_z + \frac{1}{\sqrt{3}}|-\alpha\rangle_z(|\beta\rangle_z + i|-\beta\rangle_z). \quad (38)$$

We drop the subscripts A and B , where it is clear that the first (second) ket refers to the first (second) system. We now suppose at each lab that observers may make a measurement of either σ_z (as performed by the friends), or S_y (as performed by the superobservers). The friends' measurements of σ_z are modeled by the Hamiltonians H_{Am} and H_{Bm} each of which leads to a coupling with a local meter m . Hence, we write

$$|\psi_{zz,m}\rangle_{FR} = e^{-iH_{Am}t/\hbar} e^{-iH_{Bm}t/\hbar} |\psi_{zz}\rangle_{FR}. \quad (39)$$

We give an example of H_{Am} in the Appendix. The state of the labs after the friends' measurements is given by

$$|\psi_{zz,mF}\rangle_{FR} = e^{-iH_{AmF}t/\hbar} e^{-iH_{BmF}t/\hbar} |\psi_{zz,m}\rangle_{FR}, \quad (40)$$

which describes that the friends have themselves become coupled (entangled) with the meters. The coupling is given by interactions H_{AmF} and H_{BmF} .

We suppose that both the Wigner superobservers measure S_y . The interactions H_{Am} , H_{Bm} , H_{AmF} , and H_{BmF} are reversed. The superobservers perform the respective local unitary interactions U_A^{-1} and U_B^{-1} as in (29) to change the measurement settings from z to y . After the unitary evolution corresponding to the measurement interaction, the state of the system is

$$\begin{aligned} |\psi_{yy}\rangle_{FR} &= U_A^{-1} U_B^{-1} |\psi_{zz}\rangle_{FR} \\ &= \frac{i}{2\sqrt{3}} \{-3i|\alpha\rangle_y|\beta\rangle_y - i|-\alpha\rangle_y|-\beta\rangle_y \\ &\quad + |\alpha\rangle_y|-\beta\rangle_y - |-\alpha\rangle_y|\beta\rangle_y\}. \end{aligned} \quad (41)$$

Each system is coupled to a meter M (in the superobservers' labs), using interactions H_{AM} and H_{BM} . A pointer measurement is then made so that the superobservers may record the outcomes. We see that there is a nonzero probability of 1/12 that both observers get outcomes -1 and -1 for measurements of S_y .

The alternative setup is where the friend of lab B measures σ_z and the superobserver of laboratory A measures S_y . After the reversals, and the unitary interaction U_y , the state is

$$\begin{aligned} |\psi_{yz}\rangle_{FR} &= U_A^{-1} |\psi_{zz}\rangle_{FR} \\ &= \frac{e^{i\pi/4}}{\sqrt{6}} \{2|\alpha\rangle_y|-\beta\rangle_z + |-\alpha\rangle_y|\beta\rangle_z - i|\alpha\rangle_y|\beta\rangle_z\}. \end{aligned} \quad (42)$$

The probability of getting -1 for lab B and -1 for lab A on measurements of σ_z and S_y , respectively is zero: $P_{--|yz} = 0$

The FR logic is as before: If, from (42), Wigner superobserver A gets -1 for S_y , it is inferred from the state $|\psi_{yz}\rangle_{FR}$ that the friend B is $+1$ for σ_z . But if the friend B gets the result $+1$ for σ_z , then one infers from the original state $|\psi_{zz}\rangle_{FR}$ at time t_1 [Eq. (37)] that the friend for system A measured down for σ_z .

Yet, considering measurements of σ_z at A and S_y at B , if A was in the state -1 as measured by the friend A , then there is no possibility to get outcome -1 for S_y at B . The probability

of obtaining -1 and -1 for measurements σ_z and S_y is zero. This is seen by considering the measurement of σ_z at A and S_y at B : The final state after the reversals and unitary rotation at B is written

$$\begin{aligned} |\psi_{zy}\rangle_{FR} &= U_B^{-1} |\psi_{zz}\rangle_{FR} \\ &= \frac{e^{i\pi/4}}{\sqrt{3}} \left\{ \frac{1}{\sqrt{2}} |\alpha\rangle_z (|-\beta\rangle_y - i|\beta\rangle_y) + \sqrt{2} |-\alpha\rangle_z |\beta\rangle_y \right\}. \end{aligned} \quad (43)$$

We find $P_{--|zy} = 0$. This implies the impossibility to get both outcomes of S_y being -1 at A and B , in contradiction to the earlier result. This gives the paradox for a situation where all the measurements, including those initially made by the friends, are distinguishing between two macroscopically distinct states.

IV. ANALYSIS USING MACROSCOPIC REALISM

The macroscopic version of the paradox identifies two macroscopically distinct states available to the systems at each time t_i . This gives an inconsistency in the realistic perception of the same event by the two observers, even where those events are based on measurements of macroscopic qubits, which is puzzling. Here, we examine the definitions of macroscopic realism carefully, showing that a *deterministic form of macroscopic realism* is indeed falsified by the Wigner friend paradoxes.

Macroscopic realism (MR) is the assumption that a system “which has just two macroscopically distinguishable states available to it” at the times t_k will actually be in one of those states at time t_k , prior to any measurement [27]. If we consider a system in a superposition of two macroscopically distinct states (e.g., $|\alpha\rangle$ and $|-\alpha\rangle$, as $\alpha \rightarrow \infty$), then MR posits that the outcome of a measurement (say \hat{X}) that distinguishes between those states will have a predetermined value λ prior to the measurement actually taking place. We emphasize that in the definition of MR, there is no specification of what is meant by “states.” The definition of MR that we consider is general and does *not* imply that the system be in one of the states that form the superposition (e.g., $|\alpha\rangle$ or $|-\alpha\rangle$), a result that can be negated [37]. To the best of our knowledge, there has been no direct experimental negation of the premise of MR, as defined in the general sense here. Violations of Leggett-Garg inequalities require additional assumptions linked to the premise of noninvasive measurability [27,57–59].

However, in the setups that we have proposed for the realization of the Wigner friend paradoxes using cat states, there is a consideration of different measurement settings (e.g., S_y and S_z). The operation that determines the setting occurs in the lab, as a real interaction. The operation is usually considered to be part of the measurement. For both settings, the system is in a superposition (or mixture) of macroscopically distinct states, prior to the final pointer stage of the measurement X that distinguishes the states [as in Eqs. (33)–(36)].

If the predetermination λ of the outcome for *both* measurements (e.g., S_y and S_z) is assumed to apply to the system as it exists *prior* to the part of the measurement (the dynamics U_θ) that fixes the setting (y or z), then this is a strong (more restrictive) form of MR, that we refer to as *deterministic*

macroscopic realism (dMR). This form of MR has been shown previously to be negated by quantum predictions in several different scenarios [30,32,38,60].

A. Deterministic macroscopic (local) realism falsified

Result 4.A. The violation of the Bell-Wigner inequality for the cat-state version of the experiment implies failure of deterministic macroscopic realism.

Proof. The Bell-Wigner inequality (2) would hold, if simultaneous predetermined values for both spin measurements σ_y and σ_z defined by (23) and (24) are identifiable for both systems A and B , for the state $|\psi_{zz}\rangle_{WF}$ [Eqs. (3) or (33)]. With this assumption, one would specify hidden variables λ_z^A and λ_y^A that predetermine the results of the measurements of σ_z^A and σ_y^A , respectively, and hidden variables λ_z^B and λ_y^B that predetermine the results of the measurements of σ_z^B and σ_y^B , respectively, should those measurements be performed by the friends. The values of λ_z^A , λ_y^A , λ_z^B , λ_y^B are each either $+1$ or -1 , corresponding to the value for the outcome of the respective measurements, if performed. In the setup, the possible results for each λ identify macroscopically distinct states for the system, as evident by writing the state $|\psi\rangle_{WF}$ in the respective bases, as in Eqs. (33)–(36).

Following the definitions of macroscopic realism given in Refs. [27,30,31,33,38], we then refer to the assumption of the simultaneous predetermined variables as *deterministic macroscopic realism* (dMR). The assumption naturally includes that of locality, but we may also specify the assumption as *deterministic macroscopic (local) realism* to make this clear. Following the original proofs of the Bell inequalities [5,6], the Bell-Wigner inequality follows based on the assertion of the simultaneous variables λ_z^A , λ_y^A , λ_z^B , and λ_y^B . The premise dMR also specifies that the measurements S_z and S_y of the superobservers are determined by the hidden variables λ_z and λ_y , at the respective site. The assumption of dMR is therefore falsified by the violation of the Bell-Wigner inequality. ■

B. Failure of deterministic macroscopic realism: The Frauchiger-Renner paradox

Result 4.B. The premise of dMR is also falsified by the FR paradox, where the assertion applies to the state $|\psi_{zz}\rangle_{FR}$ [Eq. (37) or (38)].

Proof. A table of all the values λ_z and λ_y that are possible for each system A and B according to dMR can be constructed. The table is given in Appendix A 3. The impossibility of consistency with the outcomes predicted by quantum mechanics is evident. The values of $\{\lambda_{zA}, \lambda_{zB}, \lambda_{yA}, \lambda_{yB}\}$ given by a row of the table represent a possible dMR state. If a spin z or a spin y measurement is made on system A , the outcome will be λ_{zA} or λ_{yA} , respectively. Similarly, λ_{zB} and λ_{yB} are the outcomes of spin z and spin y measurements if made on system B . In the table, the joint probability of the possible spin outcomes for the given dMR state is given across the row. The joint probability for the spin outcomes, given a measurement of z or y at A and B , is denoted $P_{\epsilon_A \epsilon_B | \theta \phi}$, where ϵ_A (ϵ_B) is the sign of the spin outcome at A (B), and θ and ϕ are the respective spin measurements (z or y) at A and B . The dMR states for which $P_{-|zy} = 0$ and $P_{-|yz} = 0$ [corresponding to measurements

of $\sigma_z^A \sigma_y^B$ and $S_y^A \sigma_z^B$] can be identified by examining the last two columns. There is no possibility of an FR paradox, since those states for which the result is also $-$, $-$ for measurements $S_y^A S_y^B$ are highlighted by the stars. There is only one, but this dMR state gives a nonzero probability for outcomes $++$ (both up) for $\sigma_z^A \sigma_z^B$, which is inconsistent with the initial state $|\psi_{FR}\rangle \equiv |\psi_{zz}\rangle_{FR}$. The initial state has zero probability for $++$: Therefore the predictions of the dMR state are not compatible with the state (37). The table gives a falsification of dMR, if the predictions of quantum mechanics are correct.

It is also possible to falsify dMR for the FR system, using the Bell-Wigner inequality. The choice of measurement is of either S_y or σ_z at each site. Hence we write the Bell-Wigner inequality for the two laboratories, $L_A \equiv A$ and $L_B \equiv B$ as in (2), in terms of the moments,

$$S = |\langle A_z B_z \rangle + \langle A_y B_z \rangle + \langle A_z B_y \rangle - \langle A_y B_y \rangle| \leq 2. \quad (44)$$

The assumption of dMR implies the inequality (34) (from the proof of Result 4.A). The assumption implies local hidden variables that predefine the values for A_z , A_y , B_z and B_y to each be either $+1$ or -1 , implying the existence of the joint probability $p(A_z, A_y, B_z, B_y)$ whose marginals satisfy the CHSH-Bell inequality. For the FR paradox, there are four possible preparation states: $|\psi_{zz}\rangle_{FR}$, $|\psi_{yz}\rangle_{FR}$, $|\psi_{zy}\rangle_{FR}$, and $|\psi_{yy}\rangle_{FR}$. Identifying the outcomes of σ_z^A , S_y^A , σ_z^B and S_y^B to be A_z , A_y , B_z and B_y respectively, we evaluate from these states the following:

$$\begin{aligned} \langle \sigma_z^A \sigma_z^B \rangle &= -1/3, \\ \langle S_y^A \sigma_z^B \rangle &= -2/3, \\ \langle \sigma_z^A S_y^B \rangle &= -2/3, \\ \langle S_y^A S_y^B \rangle &= 2/3, \end{aligned} \quad (45)$$

which gives a value of $S = 7/3$. The violation of the inequality falsifies dMR. ■

V. WEAK MACROSCOPIC REALISM

In this section, we show how consistency between macroscopic realism and the quantum predictions of the Wigner friends gedanken experiment can be obtained. Since deterministic macroscopic realism is falsifiable by the experiment, it is necessary to define macroscopic realism in a less strict sense, as given by a weaker (more minimal) assumption. This motivates the premise of *weak macroscopic realism* (wMR), as defined in Refs. [30,31,33]. Below, we explain how wMR can be consistent with the Wigner-friend paradoxes.

To understand the meaning of wMR, we examine the dynamics associated with the operation U_θ that fixes the measurement setting as either σ_z or σ_y depending on the time of evolution, as in Fig. 3. The dynamics reveals an evolution over timescales of order Ω , during which the system *cannot always be given as a superposition (or mixture) of the two states* $|\alpha\rangle$ and $|\neg\alpha\rangle$. Let us consider the system of Fig. 3 at the times $t_2 = \pi/2\Omega$ and $t_3 = 3\pi/2\Omega$, for which the system

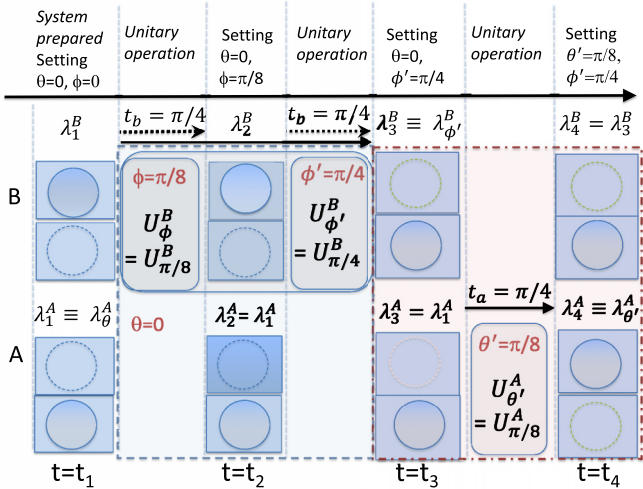


FIG. 4. The weak macroscopic realism (wMR) Assertions can be understood by considering the analogy of a ball in one of two boxes. There are two pairs of boxes, one in each lab A and B, and a ball for each pair. Each ball can be shuffled among the boxes of its pair, and the boxes then opened to determine which box each ball is in. The opening of the boxes is analogous to a measurement of spin, the choice of shuffling modeling the choice of measurement settings, θ and ϕ . Assertion wMR(1) posits that at each time t_k ($k = 1, 2, 3, 4$) after the shuffling, the ball is in one of the boxes, prior to an observer opening the boxes. The predetermined spin values are given as λ_k^A and λ_k^B . Assertion wMR(2) posits that these values cannot then be changed by any further shuffling that occurs at the other lab at a later time. For example, the value λ_1^A does not change at time t_2 or t_3 due to U_ϕ^B or $U_{\phi'}^B$ and hence $\lambda_3^A = \lambda_2^A = \lambda_1^A$. However, once further shuffling $U_{\theta'}^A$ at A occurs, to change the local setting from $\theta = 0$ to $\theta' = \pi/8$, wMR does not assert that the value $\lambda_{\theta'}^A$ cannot depend on the shuffling (U_ϕ^B or $U_{\phi'}^B$) that may have occurred at B from time t_1 to t_4 . Hence, according to wMR, the observation of any nonlocality requires rotations at both sites (indicated by the grey dashed and pink dashed-dotted rectangles).

is in such a macroscopic superposition. The assumption that the system defined *at the time* t_k ($k = 2, 3$) has (as $\alpha \rightarrow \infty$) a definite value λ_k for the outcome of the *pointer* stage of the measurement, given by the sign of the quadrature phase amplitude measurement \hat{X}_A , motivates a weak form of the macroscopic realism (MR) premise.

A. Definition of weak macroscopic realism

As with Bell tests [4], in order to justify the locality assumption used in the derivation of the inequality (2), we consider that during the experiment the laboratories of the two friends (and the associated superobservers) are spatially separated to the extent that any event or interaction that takes place for one lab cannot causally influence the events or outcomes in the second lab i.e., the labs are spacelike separated [61,62]. It is assumed that the superobservers Alice and Bob are at rest in the respective lab frames, and that there is no relative motion with respect to the two laboratories. Weak macroscopic realism (wMR) implies the following two Assertions (Fig. 4) [30,31].

1. Assertion wMR (1)

We consider the system that is prepared at the time t_k *after* the unitary dynamics U_θ that determines the measurement setting θ . The system at this time t_k is prepared with respect to the measurement basis θ , and (we suppose, as depicted in Figs. 3 and 4) is in a superposition (or mixture) of *macroscopically distinct* states that each have a definite outcome for the pointer measurement of the spin with setting θ . In the context of a general spin measurement, as in the definitions of wMR, we choose to denote the spin-component by S_θ (but emphasize the notation in this context is not intended to distinguish between the measurements of the friends and of the superobservers).

Assertion wMR(1) is that this macroscopic system, prepared *after* the local unitary dynamics U_θ , can be regarded as having a definite predetermined value λ_θ (+1 or -1) for the outcome of S_θ . In other words, macroscopic realism (MR) applies to the macroscopic system prepared in a macroscopic superposition state *after* the unitary interaction U_θ that fixes the measurement setting θ (e.g., as S_z or S_y). This value λ_θ can be considered the value of the “record” of the result of the measurement at that time, even if the final pointer stage of the measurement is not actually carried out.

We illustrate the application of Assertion wMR(1). Consider systems prepared at the time t_k in the macroscopic superposition state

$$|\psi_{zz}\rangle_{WF} = A_{zz}(|\alpha\rangle_{z,C}|\alpha\rangle_{z,D} + |-\alpha\rangle_{z,C}|-\alpha\rangle_{z,D}) + B_{zz}(|\alpha\rangle_{z,C}|-\alpha\rangle_{z,D} + |-\alpha\rangle_{z,C}|\alpha\rangle_{z,D}), \quad (46)$$

as in Eq. (33), or else in the spin-friend system

$$|\Phi\rangle_{SF} = \frac{1}{\sqrt{2}}(|\uparrow\rangle_z|F_{z+}\rangle + |\downarrow\rangle_z|F_{z-}\rangle), \quad (47)$$

as in Eq. (1). In both cases, the system can be regarded as being in superposition of macroscopic “pointer” states for spin z measurements. This is because a direct amplitude measurement of \hat{X}_A (or \hat{X}_B) for (33) or of the friend’s equipment for (1) would yield the measurement outcome for S_z^A (or S_z^B), or of σ_z , respectively. The systems are prepared at the time t_k in the measurement basis, ready for the pointer measurement: According to wMR(1), the system (46) at the time t_k can be regarded as having definite predetermined values λ_z^A, λ_z^B (being +1 or -1) for the outcomes S_z^A and S_z^B . Similarly, the system prepared in (47) has a definite value λ_z for the outcome of the spin measurement σ_z . According to wMR, the value λ_θ that at time t_k predetermines the outcome for the macroscopic spin measurement σ_θ if made by the friend is the same value that predetermines the spin measurement S_θ , if made by the superobserver. This is because there is no change of measurement setting.

2. Assertion wMR (2)

Where there are two spatially separated systems, or labs, as in the extended Wigner-friend experiments, it is necessary that the premise of weak macroscopic realism addresses how the assumption of locality applies to the hidden variables λ_θ defined for each lab system. In this context, to understand the motivation for the premise, it is useful to refer to the analogy given below, of balls shuffled among a set of boxes.

The second assumption of weak macroscopic realism [Assertion of wMR(2)] is that the value λ_θ assigned [according to Assertion wMR(1)] to the local system at the time t_k (after the local unitary interaction U_θ that fixes the local measurement setting θ) cannot *then* be changed by any event or interaction that subsequently occurs at the *other* spacelike-separated system, or lab. In other words, there is locality with respect to this pointer value λ_θ : It is assumed that the value λ_θ predetermining the outcome for the (pointer) measurement S_θ is not subsequently changed by future events or interactions U_ϕ that occur at the separated system.

B. Analogy: A ball shuffled between boxes

The Assertions of wMR are less restrictive than those of local realism introduced by Bell. The motivation for the Assertions is given by the macroscopic nature of the systems, and the role played by the unitary interactions U that fix the measurement settings. We see from Fig. 3 that the dynamics of U does not allow the application of the premise of MR at all times, because the system is not in a macroscopic superposition at all times. This motivates us to introduce an asymmetry with regard to the assumptions, which prioritizes the times when macroscopic superposition states are formed.

It is useful to consider an analogy motivated by the three-box paradox, in which a ball is placed in one of a set of boxes [63–67]. The set of boxes the ball can be in defines the macroscopically distinct states of a system. Following Refs. [33,67], we consider there are two boxes in the set. The ball can then be shuffled between the boxes, and an observer can then open the boxes to determine the state of the system (the value of λ), as in which box the ball is in. In the analogy, the local unitary operations U_θ determining the measurement setting θ correspond to particular shuffling sequences of the ball among a given set of boxes, the shuffling being a reversible process.

In our example, there are two spatially separated sets of boxes, in the different labs labelled A and B , and a ball is associated with each set (Fig. 4). The balls can be found to be in one of the boxes (if opened) of each set at the initial time t_1 . After preparation at time t_1 , there can be a shuffling at each site, corresponding to U_θ^A and U_ϕ^B . The premise of wMR(1) posits that at the time t_k^A after the shuffling has been completed at the local site A , macroscopic realism applies to the state of the ball at A , i.e., the ball is in one of the boxes at A , so that there is a predetermined value λ_k^A giving the outcome if an observer opens the boxes to determine which box the ball is in. The same is true for the ball in the second set of boxes at lab B . At the time t_j^B after the local shuffling U_ϕ^B at B , the ball is in one of the local set of boxes i.e., there is a definite value λ_j^B giving the state of the ball.

Assertion wMR(2) is a partial locality assumption. It is posited that the state of the ball at lab A at the time t_k^A (after the local shuffling U_θ^A has been completed) cannot be changed by any shuffling U_ϕ^B that *then* occurs at the other set of boxes, B . We see that the full locality assumption specified by Bell would imply that the interactions U_ϕ^B do not in any way affect the value of λ_θ^A , which is a stronger assumption. The same Assertion wMR(2) holds with respect to the ball at lab B .

It is important to note that the Assertions of wMR do not refer to the entire “state” of the system (the ball), but refer *only*

to the value of λ which gives the *macroscopic* outcome. It is only assumed that the value of λ is determined at the time t_k . For example, the state of the ball prior to and after an observer opens the boxes can be different, but have the same value of λ . It is also not assumed that the “state” of the ball at A is not affected by any shuffling occurring at B , for example, since the full “state” includes microscopic detail not specified by λ . This is discussed in Refs. [66] and [67], which address tests of macrorealism for the three-box paradox.

A similar analogy arises for a recent macroscopic realization of the Einstein-Podolsky-Rosen paradox using Bose-Einstein condensates [68]. In that experiment, the measurement setting is determined by an interaction of the atoms with a pulse. After the interaction, and just prior to a final measurement involving atom counting, the atoms can be considered to have available to them two atomic states. It can be argued that the atoms are analogous to the macroscopic balls sitting in one of two boxes, and that weak macroscopic realism applies.

For measurements of the qubit value associated with the two coherent states of system A , the final pointer stage of the measurement corresponds to the determination of the sign of the quadrature phase amplitude X_A . The premise wMR specifies a hidden variable λ_θ^A for the outcome of this pointer measurement *once* the dynamics U_θ^A associated with the choice of measurement setting has occurred. This means that the predetermination is with respect to one or other spin, e.g. S_z or S_y , not both simultaneously. For example, in Fig. 4, the assertion applies to predetermine at the time t_2 the outcomes of the spins with settings $\phi = \pi/8$ at B and $\theta = 0$ at A . For system B of Fig. 4, the assertion applies to predetermine the spin outcome for $\phi = \pi/8$ at time t_2 , and then to predetermine the outcome for $\phi = \pi/4$ at the *different* time t_3 (after the dynamics U_ϕ^B).

The assertions of wMR allow for nonlocality, as illustrated in Fig. 4. However, a careful examination reveals that the impact of any nonlocality will manifest *symmetrically*, in the sense of requiring unitary rotations (changes of measurement setting) at both sites. This has been pointed out in Refs. [30,31] and is illustrated in Figs. 4–6. As part of the definition of wMR, it is assumed in Fig. 4 that the value λ_θ^A predetermining the pointer measurement for spin S_θ^A at the time t_2 is not changed at time t_3 by the unitary rotation U_ϕ^B at B that then takes place at B . However, if there is a further local unitary rotation $U_{\theta'}^A$ at A , as in Fig. 4, then a different value $\lambda_{\theta'}^A$ applies to the system at the later time after the interaction $U_{\theta'}^A$, to predetermine the result of the new pointer measurement $S_{\theta'}^A$. The wMR postulate does not assert that this value is not affected by the unitary rotation U_ϕ^B , because here there are *two unitary rotations* from the initial time considered of t_2 , one at B and one at A . Hence, for nonlocality to be observed consistently with wMR, it is necessary to change the measurement setting at both sites.

C. Consistency of weak macroscopic realism with macroscopic Bell violations using cat states

The Assertions of wMR are less restrictive than those of Bell's local realism [3,5,7] and we show in Sec. V D2 that the Assertions do not imply Bell-CHSH inequalities. It is

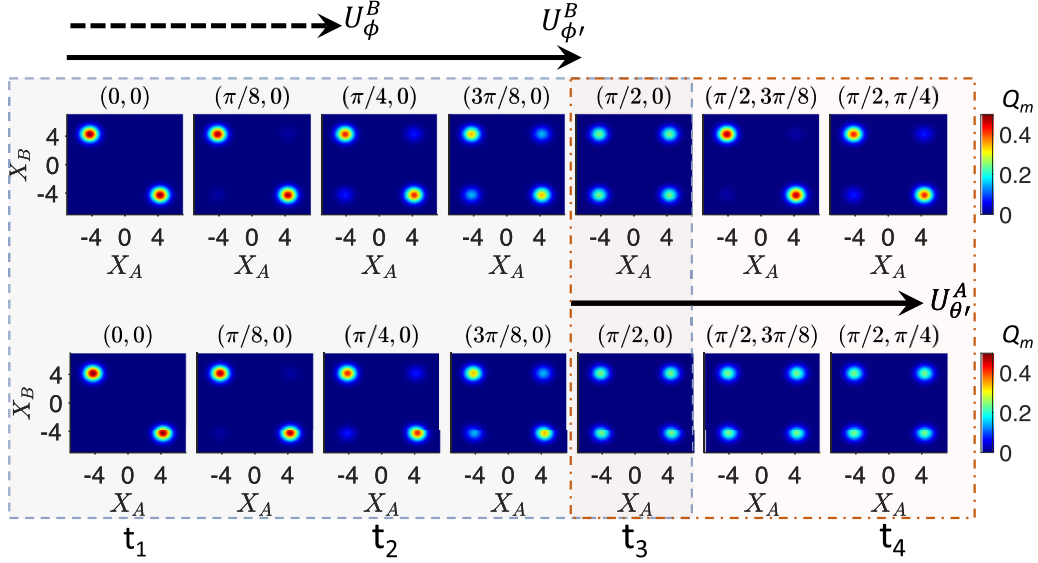


FIG. 5. The violation of the Bell inequality (52) is consistent with weak macroscopic realism (wMR). We plot the quantum dynamics for the system depicted in Fig. 4 as it evolves under the interactions H_{nl}^A and H_{nl}^B of Eq. (49) for the respective times t_a and t_b , given as (t_b, t_a) above each snapshot, in units of Ω^{-1} . The measurement settings $\theta = 0$, $\phi = \pi/8$, $\phi' = \pi/4$, and $\theta' = \pi/8$ are realized by the unitary rotations U^A and U^B , as the local system is evolved for the appropriate time. Shown are the contour plots for the marginal $Q_m \equiv Q(X_A, X_B)$ of the Q function of the quantum state as it evolves. The sign of \hat{X}_A (\hat{X}_B) at t_k gives the appropriate spin value S_j^A (S_j^B). The joint probabilities for S_1^A and S_2^B are measured at time t_2 ; those for S_1^A and S_3^B at time t_3 ; and those for S_3^B and S_2^A at time t_4 . The probabilities are indicated by the relative weighting of the peaks (refer to text). In the top sequence, the initial state is the Bell-cat state, Eq. (48) ($\alpha = 4$), and the predictions violate the Bell inequality (52). There is no inconsistency with the Assertions of wMR, which assign predetermined values for the spins according to Fig. 4, the spin values $S_1^A, S_2^B, S_3^B, S_2^A$ given by $\lambda_1^A, \lambda_2^B, \lambda_3^B, \lambda_4^A$, respectively. In the lower sequence, the initial state is the mixed state ρ_{mix} , Eq. (53), and a Bell violation is not possible. There is no distinction between the predictions for $|\psi_{\text{Bell}}\rangle$ and ρ_{mix} at times t_1, t_2 , and t_3 (gray dashed rectangle) where there is a unitary rotation at only one site, B . The predictions clearly diverge by time t_4 (pink dashed-dotted rectangle), after rotations at both sites, as is consistent with the premises of wMR.

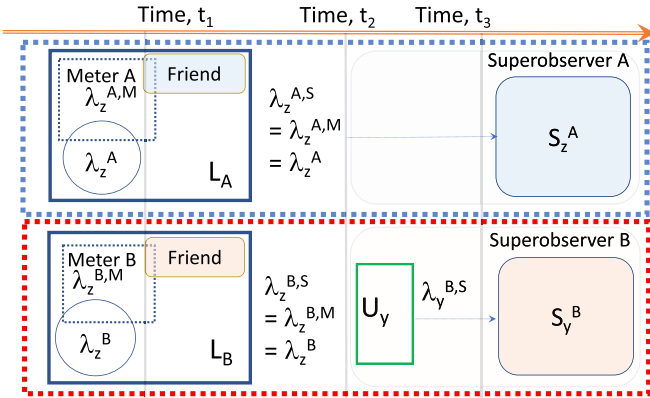


FIG. 6. The weak macroscopic realism (wMR) model. The cat systems at time t_1 are described by variables λ_z^A and λ_z^B that predetermine outcomes for measurements of σ_z . After interaction with the cat systems, the meters are attributed values $\lambda_z^{A,M}$ and $\lambda_z^{B,M}$ that predetermine the outcome of the measurement on them by the friends ($\lambda_z^{A,M} = \lambda_z^A, \lambda_z^{B,M} = \lambda_z^B$). These variables predetermine the outcomes ($\lambda_z^{A,S}$ and $\lambda_z^{B,S}$) if a measurement is made of S_z by the superobservers A or B , at the time t_2 . There is no change of measurement setting at A . Hence $\lambda_z^{A,S}$ predetermines the outcome for S_z^A by superobserver A at time t_3 , regardless of any unitary U_y at B . If superobserver B performs a unitary interaction U_y to prepare the system for a (pointer) measurement S_y , then the system at time t_3 is attributed a variable $\lambda_y^{B,S}$ that predetermines the outcome. It is now not necessarily true that the value λ_z^B predetermines the outcome of a future measurement S_z^B .

possible that a model compatible with wMR will violate Bell inequalities [30]. Here, we summarize the results of Ref. [30], which demonstrate how Bell violations can be consistent with wMR.

Consider the bipartite systems A and B prepared at time t_1 in a Bell-cat state [56]

$$|\psi_{\text{Bell}}\rangle = N(|\alpha\rangle|-\alpha\rangle - |-\alpha\rangle|\alpha\rangle). \quad (48)$$

Here, α is real, and N is the normalization constant. The nonlinear interaction

$$H_{nl}^A = \hbar\Omega\hat{n}_A^4 \quad (49)$$

[which differs from Eq. (26)] provides a unitary evolution with the property that after an interaction time $t_a = t_2 = \pi/4\Omega$, the system A if initially prepared in a coherent state $|\alpha\rangle$ evolves into the state [30]

$$U_{\pi/8}^A|\alpha\rangle = e^{-i\pi/8}(\cos \pi/8|\alpha\rangle + i \sin \pi/8|-\alpha\rangle). \quad (50)$$

Similarly, after a time $t_a = t_3 = \pi/2\Omega$, the system is in the state

$$U_{\pi/4}^A|\alpha\rangle = e^{-i\pi/4}(\cos \pi/4|\alpha\rangle + i \sin \pi/4|-\alpha\rangle). \quad (51)$$

A similar interaction $H_{nl}^B = \hbar\Omega\hat{n}_B^4$ can occur at B , with an evolution time t_b , the interaction times t_a and t_b being independently controlled at each site to determine the local measurement setting. This allows three choices of measurement setting at each site, corresponding to the choice of interactions times $t_{a/b} = 0, \pi/4\Omega, \pi/2\Omega$. Measurements of

the signs (+ or -) of the quadrature phase amplitudes \hat{X}_A and \hat{X}_B [Eq. (25)] after interacting locally for times $t_a = t_j$ and $t_b = t_k$ ($j, k = 1, 2, 3$) give outcomes of either +1 or -1, respectively, for each system, which we denote as the spin outcomes, S_j^A and S_k^B . Bell's original inequality $|\langle S_1^A S_2^B \rangle - \langle S_1^A S_3^B \rangle| \leq 1 + \langle S_2^A S_3^B \rangle$ [3] implies

$$-\langle S_1^A S_2^B \rangle + \langle S_1^A S_3^B \rangle - \langle S_2^A S_3^B \rangle \leq 1. \quad (52)$$

A violation of the Bell inequality (52) is predicted for the Bell-cat system [30]. We consider the top sequence depicted in Fig. 5, where $t_4 = 3\pi/4\Omega$. The sequence depicts the dynamics as the unitary operations associated with the spin measurements S_j are performed on $|\psi_{\text{Bell}}\rangle$. The sequence is as given in Fig. 4, where we assign the variables λ_k at each of the times t_k ($k = 1, 2, 3, 4$) according to wMR. In Fig. 5, the predictions for the Bell cat state (48) are given in the form of contour plots of the marginal $Q(X_A, X_B)$ of the Q function as the dynamics unfolds. The full two-mode Q function $Q(X_A, P_A, X_B, P_B)$ is defined as $Q = \frac{1}{\pi^2} |\langle \beta_0 | \langle \alpha_0 | \psi_{\text{Bell}} \rangle|^2$ where $\alpha_0 = X_A + iP_A$, $\beta_0 = X_B + iP_B$, and $|\alpha_0\rangle$ and $|\beta_0\rangle$ are coherent states of the fields A and B , respectively [39]. The distributions at each time show peaks corresponding to distinctly positive or negative values (4 or -4) of X_A and X_B . At $t_a = t_b = 0$, the anticorrelation is evident. The measurements of \hat{X}_A and \hat{X}_B after evolution times $t_a = 0$ and $t_b = \pi/4\Omega$ yield the moment $\langle S_1^A S_2^B \rangle$ (third snapshot from the left). Similarly, the moment $\langle S_1^A S_3^B \rangle$ is given after times $t_a = 0$ and $t_b = \pi/2\Omega$ (fifth snapshot from left), and that of $\langle S_2^A S_3^B \rangle$ after times $t_a = \pi/4\Omega$ and $t_b = \pi/2\Omega$ (final snapshot on the right). It is confirmed in Ref. [30] how (for large $\alpha > 2$) the relative weighting of the distinct peaks gives the joint probability for the spin outcomes. In fact, $\langle S_1^A S_2^B \rangle = \langle S_2^A S_3^B \rangle = -1/\sqrt{2}$, $\langle S_1^A S_3^B \rangle = 0$, which violates (52) [30].

In the Fig. 5, we also plot the predictions for the mixed state

$$\rho_{\text{mix}} = \frac{1}{2}(|\alpha\rangle\langle -\alpha| + |-\alpha\rangle\langle \alpha|) \quad (53)$$

which provides a local hidden variable theory for the system and cannot violate the Bell inequality. There is no distinguishable difference (any difference vanishes exponentially as $\alpha \rightarrow \infty$ [30]) between the predictions of $|\psi_{\text{Bell}}\rangle$ and ρ_{mix} where there is a rotation at site B (or A) only. This is consistent with Assertion wMR(2), because for ρ_{mix} , the variables λ_k^A , λ_k^B depicted in Fig. 4 can be identified [30]. This is because the mixed state ρ_{mix} is equivalent to a system probabilistically with a spin "up" or "down" at each site A , and this is not changed by a local unitary interaction at B . We see from Fig. 5 that the results for $|\psi_{\text{Bell}}\rangle$ and ρ_{mix} diverge where the *unitary rotations are over both sites*, in agreement with the analysis above in Sec. V B (refer Fig. 4).

The quantum predictions given in Fig. 5 for the Bell-cat state are consistent with Assertion wMR(1). At the given times t_k ($k = 1, 2, 3, 4$) after the unitary operations, and just prior to the measurements of X_A and X_B that would determine the values of the spins (S_j^A and S_j^B , say), the system has evolved into a macroscopic superposition $|\psi_k\rangle$ of just four states, $|\alpha\rangle|\alpha\rangle$, $|\alpha\rangle|-\alpha\rangle$, $|-\alpha\rangle|\alpha\rangle$, $|-\alpha\rangle|-\alpha\rangle$. Let us denote the respective probability amplitudes as c_i ($i = 1, 2, 3, 4$). The probabilities for outcomes S_j^A and S_j^B are indistinguishable

from those of the corresponding mixture ρ_k of the four states. In such a mixture, the system is at time t_k in just *one* of the four states, with probability $|c_i|^2$, respectively, and hence has definite predetermined spin values (refer to Result 6.A). The superposition and the mixture can be distinguished by quadrature measurements, but this requires a further unitary rotation, to measure \hat{P}_A or \hat{P}_B [37].

If we also consider the interaction time $t_4 = 3\pi/4\Omega$, the system initially in a coherent state $|\alpha\rangle$ will evolve into the state

$$U_{3\pi/8}^A |\alpha\rangle = e^{i3\pi/8} (\cos 3\pi/8 |\alpha\rangle + i \sin 3\pi/8 |-\alpha\rangle). \quad (54)$$

This allows evaluation of the CHSH-Bell inequality [5,7]

$$|E(\theta, \phi) + E(\theta', \phi) + E(\theta', \phi') - E(\theta, \phi')| \leq 2, \quad (55)$$

which becomes in our notation

$$|\langle S_1^A S_2^B \rangle + \langle S_3^A S_2^B \rangle + \langle S_3^A S_4^B \rangle - \langle S_1^A S_4^B \rangle| \leq 2. \quad (56)$$

Here $\theta = 0$ implies $t_a = t_1$, $\phi = \pi/8$ implies $t_b = t_2$, $\theta' = \pi/4$ implies $t_a = t_3$, and $\phi' = 3\pi/8$ implies $t_b = t_4$. For these choices, we find that $E(\theta, \phi) = -\cos 2(\phi - \theta)$. The predictions are $\langle S_3^A S_4^B \rangle = -\cos \pi/4$ and $\langle S_1^A S_4^B \rangle = -\cos 3\pi/4$, giving a violation of the inequality. Consistency with wMR follows as for the inequality (52), as shown in Ref. [30].

D. Weak macroscopic realism and the extended Wigner's friend paradox

Now we return to the extended Wigner's friend paradox. The assumptions of Brukner's Bell-Wigner inequality are (1) locality, (2) free choice, and (3) observer-independent facts (a record from a measurement should be a fact of the world that all observers can agree on). The violation of the inequality implies at least one of the assumptions breaks down. Our motivation is to examine how the premise of wMR can be consistent with the Wigner friend paradoxes, and the violation of the inequality. In this section, we first examine which of the above assumptions can break down in a wMR-model and which records observers will agree on. We find that for consistency with wMR, the locality assumption as defined by Bell breaks down, and also that observers will agree on certain records but not others.

1. Records in a weak macroscopic realism model

We deduce which records the observers agree on in a wMR model by examining the Assertions of wMR. We find the following results:

Result 5.D.1 (1). The friends and superobservers of a given lab agree on the friend's record of σ_z . For the superobserver, this is given by S_z . From the definition of wMR, there is a predetermination of the value that would be the record of a measurement, at a time t , after the unitary interaction U_θ that determines the measurement setting θ . Hence, in the wMR model, a definite value λ_z^A (λ_z^B) predetermines the outcome of the friend's spin measurement, σ_z , at the lab A (B), once the systems have been prepared with respect to the z basis, ready for a final pointer measurement of σ_z in each lab (refer to Figs. 6 and 7). The superobservers can make a corresponding measurement of S_z , through various mechanisms which involve coupling to meters in the superobservers' labs, but which do

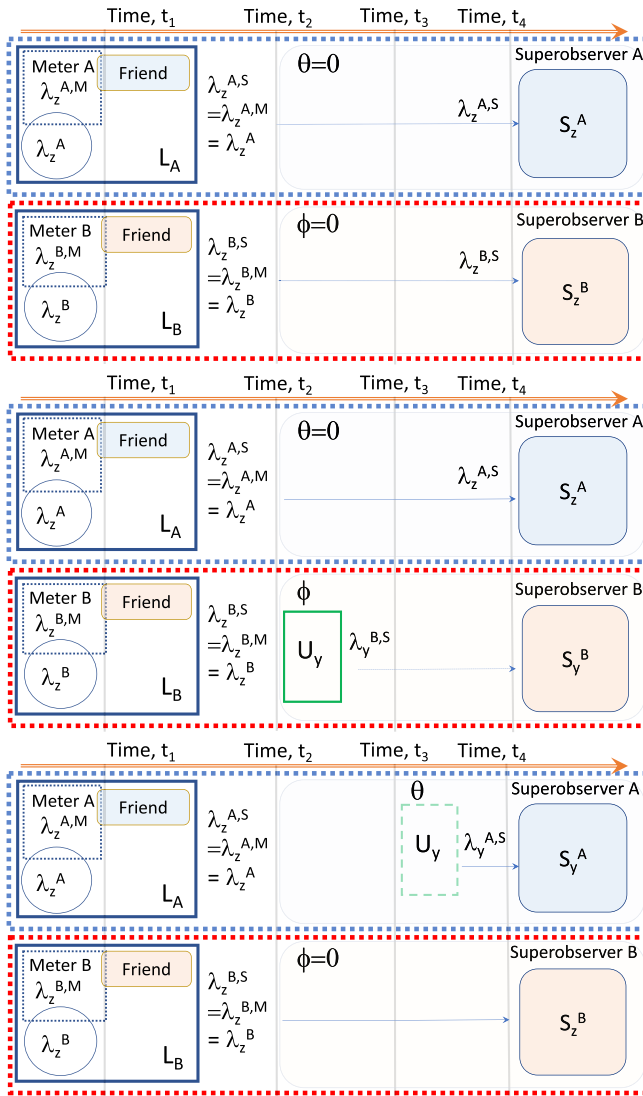


FIG. 7. Resolving the extended Wigner friend paradox for consistency with weak macroscopic realism (wMR): Partial locality. According to wMR, measuring $\langle S_z^A S_z^B \rangle$, $\langle S_z^A S_y^B \rangle$, and $\langle S_y^A S_z^B \rangle$, which (after the time t_2) require a unitary rotation at no more than one site, gives consistent records between friends and superobservers. The systems at time t_1 are prepared with respect to the basis for σ_z . The premise wMR assigns variables λ_z^A , λ_z^B , $\lambda_z^{A,M}$, and $\lambda_z^{B,M}$ to the lab systems so that $\langle S_z^A S_z^B \rangle = \langle \lambda_z^A \lambda_z^B \rangle$ (top). The superobserver B may carry out a unitary interaction U_y to prepare the system with respect to the basis Y (center). At time t_3 , the system has a definite predetermined value for S_y^B , given by $\lambda_y^{B,S}$, but the predetermination of S_z^A at site A is unaffected. Hence $\langle S_z^A S_y^B \rangle = \langle \lambda_z^A \lambda_y^{B,S} \rangle$. Similarly, $\langle S_y^A S_z^B \rangle = \langle \lambda_y^{A,S} \lambda_z^B \rangle$ (lower).

not involve a unitary interaction U that gives a change of a measurement basis. The pointer measurement made by a superobserver can be regarded as a pointer measurement on the system of the (associated) friend. In the wMR model, there is a predetermined value $\lambda_z^{A,S}$ ($\lambda_z^{B,S}$) for the outcome of the superobserver's measurement S_z^A (S_z^B), at the time t_4 , and hence the wMR model establishes that

$$\lambda_z^{A,S} = \lambda_z^A, \quad \lambda_z^{B,S} = \lambda_z^B.$$

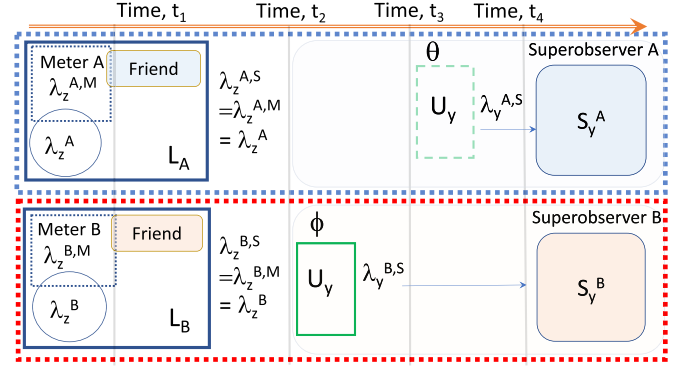


FIG. 8. Resolving the extended Wigner friend paradox for consistency with weak macroscopic realism (wMR): In the wMR model, Bell's locality need not hold, and the paradox arises, where there are two rotations after the preparation, one at each site. The system is prepared at time t_2 for pointer measurements of S_z at each site. The premise of wMR assigns variables λ to predetermine the outcome after the unitary rotations that determine the measurement settings, θ and ϕ . This means that when there are two unitary interactions U_y from the time of preparation as in the measurement of $\langle S_y^A S_y^B \rangle$ depicted in the diagram, the premise of wMR does not specify that the value of $\lambda_y^{A,S}$ (defined after $\lambda_y^{B,S}$) is independent of ϕ , and the records are not necessarily consistent according to the inequality (8). This is consistent with Fig. 5, where it is seen that the Bell nonlocality emerges for the moment $\langle S_z^A S_z^B \rangle$ which involves two rotations θ' and ϕ' , one at each site.

The value that gives the record of the friend in a given lab also gives the outcome that would be obtained for the measurement made by the associated superobserver, if they choose to measure the same spin, S_z , as the friends (i.e. they do not perform a further interaction giving a change of basis) (Figs. 6 and 7). There is agreement for these records.

Result 5.D.1 (2). There is consistency of records between the friends and superobservers, if only *one* superobserver measures a different spin component from that measured by the friends. This is because according to Assertion 2 of wMR, there is no change to the value of λ_z^A (which gives the record of σ_z^A and S_z^A) due to a further unitary interaction that takes place at B to change the local superobserver's setting from z to y at B. Similarly, there is no change to λ_z^B due to a further unitary interaction that may take place at site A. In the wMR model, the inconsistency arises where the two superobservers *both* measure a different spin (e.g., S_y). This is due to the unitary interactions U that change the measurement settings. We illustrate this in Sec. V D2 below.

2. Results about locality in a weak macroscopic realism model

The assumption of wMR implies only a partial locality. There is locality with respect to the *pointer values* λ_z once they are defined, *after* the unitary interaction U_θ . However, wMR does not imply locality (as defined by Bell [3,5,7]) in the full sense. For example, in Fig. 8, it cannot be assumed that the future outcome of S_y^A at one lab (as to be measured *after* the local unitary interaction U_y^A needed for the measurement setting) is independent of the change in measurement choice ϕ that has occurred at the other lab. We

have seen from Sec. V C by an example that Bell nonlocality can be consistent with the wMR Assertions (Fig. 5). The feature evident in Fig. 5 is that the moments contributing to the violation are those of $E(\theta', \phi') \equiv \langle S_{\theta'}^A S_{\phi'}^B \rangle \equiv \langle S_2^A S_3^B \rangle$, for which there are unitary rotations $U_{\theta'}^A$ and $U_{\phi'}^B$ giving a change of measurement setting θ' and ϕ' at both locations A and B . Here, we outline explicitly how the observed violations of the Bell-Wigner inequality are not inconsistent with wMR. We prove the following:

Result 5.D.2. Weak macroscopic realism (wMR) does not imply the Bell-Wigner and Bell-CHSH inequalities.

Proof. The Bell-Wigner inequality (8) is derived for the Wigner friend setup by noting the variables λ_z^A , λ_y^A , λ_z^B , and λ_y^B that in the derivation denote the outcomes (records) for the spins have the values either +1 or -1, which bounds the quantity

$$\lambda_z^A \lambda_z^B + \lambda_y^A \lambda_z^B + \lambda_z^A \lambda_y^B - \lambda_y^A \lambda_y^B \quad (57)$$

to have a magnitude less than or equal to 2. The derivation considers that these values exist in any single run, so that the bound corresponds to that for the averages. Bell's locality is assumed, implying that the values at any one site are independent of any change of setting at the other site. In the top diagram of Fig. 7, we can assign the values $\lambda_z^A(t_2) \equiv \lambda_z^A$ and $\lambda_z^B(t_2) \equiv \lambda_z^B$ at time t_2 , so that

$$\langle S_z^A S_z^B \rangle = \langle \lambda_z^A(t_2) \lambda_z^B(t_2) \rangle = \langle \lambda_z^A \lambda_z^B \rangle. \quad (58)$$

We then consider the center diagram, and define $\lambda_y^B(t_3) \equiv \lambda_y^B(t_3|\theta = 0)$ as the value predetermining S_y^B , where there is no rotation U_A at A . According to wMR, the pointer measurement value at A is not affected by U_B so that

$$\langle S_z^A S_y^B \rangle = \langle \lambda_z^A \lambda_y^B(t_3) \rangle = \langle \lambda_z^A \lambda_y^B \rangle. \quad (59)$$

Similarly, we consider the lower diagram and define $\lambda_y^A(t_4) \equiv \lambda_y^A(t_4|\phi = 0)$ so that

$$\langle S_y^A S_z^B \rangle = \langle \lambda_y^A(t_4) \lambda_z^B \rangle = \langle \lambda_y^A \lambda_z^B \rangle. \quad (60)$$

Figure 8 shows one way to measure the moment $\langle S_y^A S_y^B \rangle$. The value of $\lambda_y^B(t_3)$ determines S_y^B independently of the future choice of θ according to wMR because the value of the pointer measurement is specified at the time t_3 after the rotation U_y . We define $\lambda_y^A(t_4|\phi \neq 0)$ and $\lambda_y^B(t_3)$ and we can say

$$\langle S_y^A S_y^B \rangle = \langle \lambda_y^A(t_4|\phi) \lambda_y^B(t_3) \rangle = \langle \lambda_y^A \lambda_y^B \rangle. \quad (61)$$

However, the postulate of wMR is not sufficient to allow full assumption of Bell's locality: We *cannot* assume in this case that the value $\lambda_y^A(t_4) = \lambda_y^A(t_4|\phi)$ is independent of the change ϕ of the measurement setting that has occurred at B . This leads us to conclude consistency of values (records) for the measurements carried out where there is no more than one unitary rotation (as in Fig. 7), but not necessarily where there are *two* changes of measurement setting, as in the measurement of $\langle S_y^A S_y^B \rangle$ (Fig. 8). The full assumption of Bell's locality is not applicable in a wMR model, and the Bell-Wigner inequality (8) cannot be derived. A similar reasoning implies that the standard Bell inequalities (52), (55) and (56) are not implied by wMR [31,33].

A similar conclusion is reached if the moment $\langle S_y^A S_y^B \rangle$ is measured with a different time order of the unitary operations, so that the change of setting at A precedes that at B . If the interactions U_y^A and U_y^B occur simultaneously over the same time interval, then wMR posits that the values $\lambda_y^B(t_4)$ and $\lambda_y^A(t_4)$ are fixed after both interactions at time t_4 , but there is no assumption that either value is independent of the change in settings, θ and ϕ . ■

VI. CONSISTENCY OF THE QUANTUM PREDICTIONS WITH WEAK MACROSCOPIC REALISM: MACROSCOPIC WIGNER'S FRIEND AND FRAUCHIGER-RENNER PARADOXES

In this section, we explicitly show that the quantum predictions giving the macroscopic Wigner's friend and Frauchiger-Renner (FR) paradoxes are consistent with the two assertions of the wMR premise, as stated by the definition in Sec. V A. The first assertion is that the system prepared (after the unitary dynamics that determines the measurement setting) for the pointer measurement has a predetermined outcome λ . The second assertion is that this value is not altered by the subsequent dynamics at a different site. As in Sec. V C where we examine Bell violations, we show the consistency by comparing the quantum predictions with those of certain mixed states that satisfy the wMR assertions.

We will illustrate with figures for the FR paradox. Here, the system is prepared at time t_1 in the state $|\psi_{zz}\rangle_{FR}$ given by (38). It will be useful to depict the measurement dynamics associated with the unitary rotations U_θ performed on each system in terms of the Q function. The single-mode Q function $Q(\alpha_0) = \frac{1}{\pi} |\langle \alpha_0 | \psi \rangle|^2$ defines the quantum state $|\psi\rangle$ uniquely as a positive probability distribution [39]. The Q function of the two-mode state $|\psi_{zz}\rangle_{FR}$ is $Q_{zz}(X_A, P_A, X_B, P_B)$, where

$$\begin{aligned} Q_{zz} &= \frac{1}{\pi^2} |\langle \beta_0, \alpha_0 | \psi_{zz} \rangle|^2 \\ &= \frac{e^{-|\alpha|^2 - |\alpha_0|^2 - |\beta|^2 - |\beta_0|^2}}{3\pi^2} \{ e^{-2\alpha X_A - 2\beta X_B} \\ &\quad + 2 \cosh(2\alpha X_A - 2\beta X_B) + 2 \cos(2\alpha P_A - 2\beta P_B) \\ &\quad - 2e^{-2\beta X_B} \sin(2\alpha P_A) - 2e^{-2\alpha X_A} \sin(2\beta P_B) \}. \quad (62) \end{aligned}$$

Here, $\alpha_0 = X_A + iP_A$, $\beta_0 = X_B + iP_B$, and we consider α , β to be real. The first two terms in brackets give three distinct Gaussian peaks corresponding to the three outcomes for the joint spins originating from $|\alpha\rangle|-\beta\rangle$, $|-\alpha\rangle|\beta\rangle$, and $|-\alpha\rangle|-\beta\rangle$ in (38). These terms constitute the Q function of the mixture $\rho_{zz,FR}$ of the three states. The function Q_{zz} has three sinusoidal terms, which distinguish the superposition $|\psi_{zz}\rangle_{FR}$ from the mixture $\rho_{zz,FR}$. The Q function corresponds to the antinormally ordered operator moments. We may compare with the probability distribution $P(\mathbf{X}_A, \mathbf{X}_B)$ for detecting outcomes \mathbf{X}_A and \mathbf{X}_B of measurements of \hat{X}_A and \hat{X}_B . While the peaks of the marginal function $Q_{zz}(X_A, X_B)$ (defined by integrating $Q_{zz}(X_A, P_A, X_B, P_B)$ over P_A and P_B) will show extra noise, this noise is at the vacuum level. Here, we consider superpositions of macroscopically distinct coherent states, as in $|\psi_{zz}\rangle_{FR}$ [Eq. (38)], where α and β become large, and the peaks are

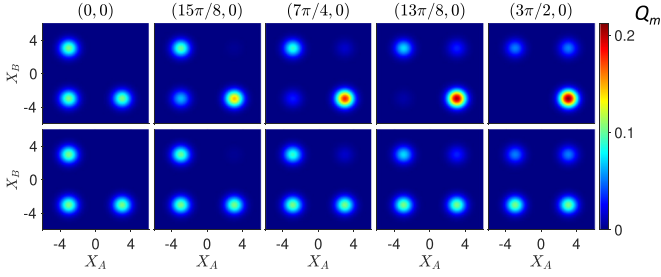


FIG. 9. Contrasting the dynamics for the system prepared in the superposition state $|\psi_{zz}\rangle_{FR}$ (top sequence) with that for the system prepared in the mixed state $\rho_{zz,FR}$ (lower sequence). The states are initially indistinguishable but become macroscopically distinguishable under evolution. In the top sequence, from left to right, we show contour plots of the marginal $Q_m \equiv Q(X_A, X_B)$ of the Q function at the times (t_a, t_b) , after the system has undergone a local evolution under H_{NL}^A and H_{NL}^B [Eq. (26)] at each subsystem (lab) A and B respectively, for the respective times t_a and t_b . The system begins in $|\psi_{zz}\rangle_{FR}$ [Eq. (38)] (top, far left) and evolves to $|\psi_{yz}\rangle_{FR}$ [Eq. (42)] (top, far right). In the lower sequence, the system begins in $\rho_{zz,FR}$ [Eq. (63)] (far left) and is evolved as for the top plots. Here, $\alpha = 3$, $\Omega = 1$.

clearly distinguishable, and identifiable as corresponding to the peaks of $P(\mathbf{X}_A, \mathbf{X}_B)$. The marginal of the Q function hence depicts the joint probability for the outcomes of the pointer measurements if made at that time.

At the special times t_k , after the unitary operations U_θ relevant to the macroscopic paradoxes have been performed, the system remains expressible as a superposition of macroscopically distinct states (refer to Fig. 3 and the model given by Fig. 4). The Q functions for the system defined at these times have macroscopic components and sinusoidal features similar to Eq. (62). The relevant spin measurements σ_θ or S_θ made at times t_k will bin the amplitudes \hat{X}_A and \hat{X}_B according to sign. As with Eq. (62), the sinusoidal terms decay with large α , β , and the joint probability for the spins if directly measured at the time t_k (without further unitary transformation) is determined by the weighting of the distinct Gaussian peaks in the Q function at the time t_k [30]. For large α , β , these peaks and their relative weightings become evident from the plots of the marginal Q functions, $Q(X_A, X_B)$ defined at the times t_k . This is evident in the Figs. 9–12.

A. Measuring S_z^A and S_z^B : Consistency with weak macroscopic realism

We first show consistency of the predictions for $\langle \sigma_z^A \sigma_z^B \rangle$ and $\langle S_z^A S_z^B \rangle$ with a wMR model, thereby verifying the first part of the definition of wMR. Consider the system prepared at time t_1 in the state $|\psi_{zz}\rangle_{FR}$. The preparation is with respect to the σ_z (S_z) “pointer basis” at each lab, so that a pointer measurement is all that is needed to complete the measurement of σ_z (S_z).

Result 6.A. The system $|\psi_{zz}\rangle_{FR}$ as prepared for the spin z pointer measurements gives predictions consistent with a wMR model.

Proof. The essential feature of the proof is the comparison between the predictions of the superpo-

sition as written in the pointer basis with that of the corresponding *mixed* state. With reference to a general state of the form $|\psi_{zz}\rangle = c_{11}|\alpha\rangle|\beta\rangle + c_{12}|\alpha\rangle|-\beta\rangle + c_{21}|-\alpha\rangle|\beta\rangle + c_{22}|-\alpha\rangle|-\beta\rangle$, the corresponding mixed state is

$$\rho_{zz} = \sum_{ij} |c_{ij}|^2 \rho_{ij}, \quad (63)$$

where $\rho_{11} = |\alpha\rangle|\beta\rangle\langle\beta|\langle\alpha|$, $\rho_{12} = |\alpha\rangle|-\beta\rangle\langle-\beta|\langle\alpha|$, $\rho_{21} = |-\alpha\rangle|\beta\rangle\langle\beta|\langle-\alpha|$, and $\rho_{22} = |-\alpha\rangle|-\beta\rangle\langle-\beta|\langle-\alpha|$. The predictions of $|\psi_{zz}\rangle$ and ρ_{zz} for the joint probabilities of the pointer measurements σ_z^A and σ_z^B are identical. The premise of wMR asserts that hidden variables λ_z^A and λ_z^B are valid to predetermine the outcome of the pointer measurements σ_z^A and σ_z^B , respectively. This interpretation holds for the mixed state ρ_{zz} , which describes a system that is indeed *in one or other* of the states comprising the mixture, and hence describable by such variables λ_z^A and λ_z^B at the time t_1 . Hence, since the predictions for the *pointer* measurement on $|\psi_{zz}\rangle$ are identical, a wMR model exists to describe the (pointer) predictions for a state of the form $|\psi_{zz}\rangle$. ■

It is useful to visualize this result for the macroscopic system by examining the Q function, where one includes the systems’ meters. Consider $|\psi_{zz}\rangle_{FR}$ given by (38). The Q function for the state (39) where the meters are explicitly included is similar to (62), but with four modes. The state is expanded as

$$\begin{aligned} |\psi_{zz,m}\rangle_{FR} &= \frac{1}{\sqrt{3}} |\alpha\rangle_z |\gamma\rangle_{Am} |-\beta\rangle_z |-\gamma\rangle_{Bm} \\ &+ \frac{1}{\sqrt{3}} |-\alpha\rangle_z |-\gamma\rangle_{Am} (|\beta\rangle_z |\gamma\rangle_{Bm} \\ &+ i |-\beta\rangle_z |-\gamma\rangle_{Bm}), \end{aligned} \quad (64)$$

where $|\gamma\rangle$, $|-\gamma\rangle$ are coherent states for the meter of the friend’s systems. We take γ as large and real. The Q function is $Q_{zz,m} = \frac{1}{\pi^4} |\langle \beta_0, \alpha_0, \gamma_A, \gamma_B | \psi_{zz,m} \rangle_{FR}|^2$. Defining the complex variables $\gamma_A = X_{\gamma A} + iP_{\gamma A}$ for the meter mode Am of system A , and $\gamma_B = X_{\gamma B} + iP_{\gamma B}$ for the meter mode Bm of system B , we find $(\alpha_0 = X_A + iP_A, \beta_0 = X_B + iP_B)$

$$\begin{aligned} Q_{zz,m} &= \frac{e^{-|\alpha|^2 - |\beta|^2 - 2|\gamma|^2}}{3\pi^4} e^{-|\alpha_0|^2 - |\beta_0|^2 - |\gamma_A|^2 - |\gamma_B|^2} \\ &\times \left\{ e^{-2\alpha X_A - 2\gamma X_{\gamma A}} e^{-2\beta X_B - 2\gamma X_{\gamma B}} \right. \\ &+ 2 \cosh(2\alpha X_A + 2\gamma X_{\gamma A} - 2\beta X_B - 2\gamma X_{\gamma B}) \\ &+ 2 \cos(2\alpha P_A + 2\gamma P_{\gamma A} - 2\beta P_B - 2\gamma P_{\gamma B}) \\ &- 2e^{-2\beta X_B - 2\gamma X_{\gamma B}} \sin(2\alpha P_A + 2\gamma P_{\gamma A}) \\ &\left. - 2e^{-2\alpha X_A - 2\gamma X_{\gamma A}} \sin(2\beta P_B + 2\gamma P_{\gamma B}) \right\}. \end{aligned} \quad (65)$$

The last three terms decay as $e^{-|\gamma|^2}$ and so, for large γ , the solution is

$$\begin{aligned} Q_{zz,m} &= \frac{e^{-P_A^2 - P_B^2 - P_{\gamma A}^2 - P_{\gamma B}^2}}{3\pi^4} \\ &\times \left\{ e^{-(X_A + \alpha)^2} e^{-(X_B + \beta)^2} e^{-(X_{\gamma A} + \gamma)^2} e^{-(X_{\gamma B} + \gamma)^2} \right. \\ &+ e^{-(X_A - \alpha)^2} e^{-(X_B + \beta)^2} e^{-(X_{\gamma A} - \gamma)^2} e^{-(X_{\gamma B} + \gamma)^2} \\ &\left. + e^{-(X_A + \alpha)^2} e^{-(X_B - \beta)^2} e^{-(X_{\gamma A} + \gamma)^2} e^{-(X_{\gamma B} - \gamma)^2} \right\}. \end{aligned} \quad (66)$$

The final meter (pointer) measurement corresponds to the measurement of the meter quadrature amplitudes, denoted as $\hat{X}_{\gamma A}$ and $\hat{X}_{\gamma B}$. The marginal $Q_{zz,m}(X_{\gamma A}, X_{\gamma B})$ describes the distribution for the measured meter outputs (as measured by the friends) and is found by integrating over all system variables as well as $P_{\gamma A}$ and $P_{\gamma B}$: We find

$$Q_{zz,m}(X_{\gamma A}, X_{\gamma B}) = \frac{1}{3\pi} \left\{ e^{-(X_{\gamma A} + \gamma)^2 - (X_{\gamma B} + \gamma)^2} + e^{-(X_{\gamma A} - \gamma)^2 - (X_{\gamma B} + \gamma)^2} + e^{-(X_{\gamma A} + \gamma)^2 - (X_{\gamma B} - \gamma)^2} \right\}. \quad (67)$$

The three Gaussians are well-separated peaks, which represent the three distinct sets of outcomes, as expected from the components of $|\psi_{zz}\rangle_{FR}$ [Eq. (38)].

The function $Q_{zz,m}(X_{\gamma A}, X_{\gamma B})$ gives the probabilities for detection of each component, for the measurement on the meter made by the friends. We see this corresponds to the marginal $Q_{\rho_{zz}}(X_A, X_B)$ of the mixed state $\rho_{zz,FR}$ (of the type (63))

$$\rho_{zz,FR} = \frac{1}{3}(\rho_1 + \rho_2 + \rho_3), \quad (68)$$

where $\rho_1 = |\alpha\rangle\langle -\beta| \langle \alpha| \langle -\beta|$, $\rho_2 = |-\alpha\rangle\langle \beta| \langle -\alpha| \langle \beta|$, and $\rho_3 = |-\alpha\rangle\langle -\beta| \langle -\alpha| \langle -\beta|$, once we put $X_{\gamma A} = X_A$ and $X_{\gamma B} = X_B$ in (67). This is expected, since the meter outcomes are a measurement of the system amplitudes \hat{X}_A and \hat{X}_B .

We may further compare the distribution (67), which describes the final outputs of the meter-measurements made by the friends, with that of the marginal Q function

$$Q_{zz}(X_A, X_B) = \frac{e^{-|\alpha|^2 - X_A^2 - |\beta|^2 - X_B^2}}{3\pi} \left\{ e^{-2\alpha X_A - 2\beta X_B} + 2 \cosh(2\alpha X_A - 2\beta X_B) + 2e^{-\alpha^2 - \beta^2} \right\} \quad (69)$$

obtained directly from the superposition $|\psi_{zz}\rangle_{FR}$ [Eq. (38)]. This is derived from Q_{zz} [Eq. (62)] by integrating over P_A and P_B . This function corresponds to that of the systems A and B prior to coupling to the meter, and gives an alternative way to model the measurement by the friends. We see that, for large $\alpha = \beta$, the last term vanishes, which gives the result for $Q_{zz}(X_A, X_B)$ identical to (67) upon replacing $X_{\gamma A}$ and $X_{\gamma B}$ with X_A and X_B . This implies that in fact for the cat state where α and β are large, the distribution for the outcomes of the *pointer measurement* on the superposition is indistinguishable from that for the outcomes of the pointer measurement made on the mixed state. This is evident from Fig. 9. The function $Q_{zz}(X_A, X_B)$ of (69) is plotted in Fig. 9 (far left top snapshot) and is indistinguishable from (67) of the mixture $\rho_{zz,FR}$ (far left lower snapshot, where $X_{\gamma A}$ and $X_{\gamma B}$ are labeled X_A and X_B).

In summary, the Q function solutions for the cat and meter states give a convincing illustration of Result 6.A, that there is consistency with wMR for $\langle \sigma_z^A \sigma_z^B \rangle$, the measurements made by the friends. The marginal Q functions $Q_{zz,m}(X_{\gamma A}, X_{\gamma B})$ and $Q_{zz}(X_A, X_B)$ for $|\psi_{zz}\rangle_{FR}$ at time t_1 are indistinguishable from those of $\rho_{zz,FR}$. Hence, the predictions for the *pointer measurements* of σ_z^A and σ_z^B on the system prepared in $|\psi_{zz}\rangle_{FR}$ at time t_1 are consistent with a wMR model. We see, however, from Fig. 9 that with an appropriate evolution, despite that the distinction between the Q functions for $|\psi_{zz}\rangle_{FR}$ and $\rho_{zz,FR}$

decays with $e^{-\alpha^2}$, the evolved states show a consistent macroscopic difference, even as $\alpha \rightarrow \infty$.

So far, the analysis concerns the measurements $\langle \sigma_z^A \sigma_z^B \rangle$ made by the friends. We now consider $\langle S_z^A S_z^B \rangle$ as measured by the superobservers. If the system-meter state given by $|\psi_{zz,m}\rangle_{FR}$ [Eq. (39)] is coupled to the friends, then the final state is written as

$$|\psi_{zz,mF}\rangle_{FR} = \frac{1}{\sqrt{3}} |\alpha\rangle_z |\gamma\rangle_{AmF} |-\beta\rangle_z |-\gamma\rangle_{BmF} + \frac{1}{\sqrt{3}} |-\alpha\rangle_z |-\gamma\rangle_{AmF} (|\beta\rangle_z |\gamma\rangle_{BmF} + i|-\beta\rangle_z |-\gamma\rangle_{BmF}), \quad (70)$$

where $|\pm\gamma\rangle_{AmF} = |\gamma\rangle_{Am}|F\rangle_A$ and $|\pm\gamma\rangle_{BmF} = |\gamma\rangle_{Bm}|F\rangle_B$ represent the combined states of the meter and friend in each lab. The measurements S_z made by the superobservers correspond to measurements on the system in a state of type (64), except that the meter systems are further coupled to second-larger meters (e.g., the friends). Since *only a pointer measurement* is necessary to complete the measurement of S_z , the final marginal distribution $Q_{zz,mF}(X_{\gamma FA}, X_{\gamma FB})$ for the outcomes of the superobservers, found after integration of the full Q function over the unmeasured variables, is identical to (67), the distribution for the mixed state $\rho_{zz,FR}$ (once we put $X_{\gamma FA} = X_A$ and $X_{\gamma FB} = X_B$). Hence by the same argument given above in the proof of Result 6.A, the distribution and predictions for the final outcomes S_z^A and S_z^B measured by the superobservers are consistent with the variables $\lambda_z^{A,S}$ and $\lambda_z^{B,S}$ defined in Result 5.D.1 (Fig. 6) that predetermine the outcomes for the superobservers, hence giving consistency with wMR.

Moreover, we prove consistency with Result 5.D.1 (1) of wMR, that the variables λ_z^A and λ_z^B predetermining the outcomes of σ_z^A and σ_z^B for the friends *are equal* to those ($\lambda_z^{A,S}$ and $\lambda_z^{B,S}$) predetermining the outcomes of S_z^A and S_z^B for the superobservers (Fig. 6):

$$\lambda_z^{A,S} = \lambda_z^{A,m} = \lambda_z^A, \quad \lambda_z^{B,S} = \lambda_z^{B,m} = \lambda_z^B. \quad (71)$$

We follow the arguments above given for Result 6.A to note that the function $Q_{zz,mF}(X_{\gamma FA}, X_{\gamma FB})$ will be indistinguishable from that obtained if the system had been prepared in the mixture $\rho_{zz,FR}$ at time t_1 , and then measured by the friends and/or superobservers. Such measurements on ρ_{zz} will satisfy (71). To prove this, consider the system prepared in ρ_{zz} . Here, one can assign variables λ_z^A and λ_z^B which indicate the system to be *in* one of the three states ρ_i [of Eq. (68)]. This implies predetermined outcomes for the spins σ_z^A and σ_z^B , consistent with wMR. If the friends make a measurement on this system, the solution is given precisely by (66). The combined system after the coupling to the meters is the correlated mixed state

$$\rho_{\text{mix},m} = \frac{1}{3}(\rho_1 \rho_{\gamma 1} + \rho_2 \rho_{\gamma 2} + \rho_3 \rho_{\gamma 3}), \quad (72)$$

where $\rho_{\gamma i}$ is the state of the meters. For the mixture, it is valid to say that if the system were in the state ρ_i at time t_1 , then the meter after the coupling is in state $\rho_{\gamma i}$. Here, because the combined system is a mixed state, one can assign variables $\lambda_z^{A,m}$ and $\lambda_z^{B,m}$ to the meters, these variables predetermining

the outcomes of the measurements on the meter. For the mixed state, the meter variables are correlated with λ_z^A and λ_z^B , those of the systems. The outcomes of the friend's measurements on the meters indicates the values of the λ_z^A and λ_z^B . Hence, we put $\lambda_z^{A,m} = \lambda_z^A$ and $\lambda_z^{B,m} = \lambda_z^B$.

We then consider the system-meter-friend state $|\psi_{zz,mF}\rangle$ given by (70). On the other hand, if the system in the mixed state $\rho_{\text{mix},m}$ is coupled to another set of meters (the friends), then the system is described by

$$\rho_{\text{mix},mF} = \frac{1}{3}(\rho_1\rho_{\gamma F1} + \rho_2\rho_{\gamma F2} + \rho_3\rho_{\gamma F3}), \quad (73)$$

which is a mixture of the three components in (70), each $\rho_{\gamma Fi}$ being a state of a meter and friend. As above, the relevant marginal Q distributions for $|\psi_{zz,mF}\rangle_{FR}$ and $\rho_{\text{mix},mF}$ that give the predictions for the pointer measurements (the outcome for spin z) are indistinguishable. One may assign variables to the system (73), these variables predetermining the outcome of the superobservers' measurements, so that (71) holds. Hence, for the system originally prepared in $\rho_{zz,FR}$, the distributions and predictions for the measurements σ_z made by the friends and S_z made by the superobservers are consistent with (71): Since these distributions and predictions are indistinguishable from those for the system prepared in $|\psi_{zz}\rangle_{FR}$, we conclude there is consistency of the predictions of the moment $\langle S_z^A S_z^B \rangle$ with (71). The measurements made by the superobservers, if they measure S_z , will be consistent with the records λ_z^A and λ_z^B obtained by the friends.

B. Measuring S_y : Consistency of the unitary dynamics with weak macroscopic realism

We next examine the measurements needed for moments such as $\langle S_y^A \sigma_z^B \rangle$, $\langle \sigma_z^A S_y^B \rangle$, and $\langle S_y^A S_y^B \rangle$. For $\langle S_y^A \sigma_z^B \rangle$ and $\langle \sigma_z^A S_y^B \rangle$, the system is prepared for the pointer measurement of σ_z (or S_z) at the time t_1 in one of the labs, but a unitary rotation U_y needs to be applied for the lab at the other site (Figs. 7 and 8). The premise of wMR asserts a value λ_z which predetermines the outcome for σ_z (or S_z). This value applies to the system from the time t_1 , and is unaffected by the dynamics U_y at the other lab. In this subsection, we show consistency with this assertion.

Result 6.B (1). Consider a system prepared in each lab A and B in the measurement basis of spin z , ready for the pointer measurement of σ_z (or S_z), which we choose to be spin z . The predictions where there is a single further rotation U_y (as defined in Sec. III C) in one of the labs will be consistent with wMR.

Proof. We are considering a state of the type

$$|\psi_{zz}\rangle = a_+|\beta\rangle|\psi\rangle_{A+} + a_-|-\beta\rangle|\psi\rangle_{A-}, \quad (74)$$

where $|\psi\rangle_{A+} = c_+|\alpha\rangle + c_-|-\alpha\rangle$ and $|\psi\rangle_{A-} = d_+|\alpha\rangle + d_-|-\alpha\rangle$, with probability amplitudes a_{\pm} , c_{\pm} , and d_{\pm} . The state (74) is written in the measurement basis, in terms of states with a definite outcome for σ_z . After a unitary rotation U_y^A at A ,

$$|\psi_{zz}(t)\rangle = a_+|\beta\rangle U_y^A(t)|\psi\rangle_{A+} + a_-|-\beta\rangle U_y^A(t)|\psi\rangle_{A-}. \quad (75)$$

The rotations give solutions of the form (refer Sec. III C)

$$\begin{aligned} |\psi_{zz}(t)\rangle = & a_+|\beta\rangle(c_1(t)|\alpha\rangle + c_2(t)|-\alpha\rangle) \\ & + a_-|-\beta\rangle(d_1(t)|\alpha\rangle + d_2(t)|-\alpha\rangle). \end{aligned} \quad (76)$$

We first show that the predictions are indistinguishable from those of the system prepared in the mixture

$$\rho_{\text{mix},B} = p_+|\beta\rangle\langle\beta|\rho_{A+} + p_-|-\beta\rangle\langle-\beta|\rho_{A-}, \quad (77)$$

where $p_+ = |a_+|^2$ and $p_- = |a_-|^2$, $\rho_{A\pm}$ being the density operator for the state $|\psi\rangle_{A\pm}$ respectively. The mixture evolves under U_y^A into

$$\begin{aligned} \rho_{\text{mix},B}(t) = & p_+|\beta\rangle\langle\beta|U_A\rho_{A+}U_A^\dagger \\ & + p_-|-\beta\rangle\langle-\beta|U_A\rho_{A-}U_A^\dagger. \end{aligned} \quad (78)$$

Upon expansion, it is straightforward to show that the measurable joint probabilities for the outcomes of σ_z^B and σ_y^A are identical to those of the evolved state $|\psi_{zz}(t)\rangle$.

The second part of the proof is to show equivalence to wMR. Here, there is preparation for the pointer measurement of σ_z^B and no further unitary dynamics occurs at lab B . Weak macroscopic realism implies a predetermined value λ_z^B for the result of S_z^B , and that this value is not affected by the unitary dynamics U_y^A that occurs in lab A . For the mixture $\rho_{\text{mix},B}$, the system B is in one or other of the states, $\rho_1 = |\beta\rangle\langle\beta|$ or $\rho_2 = |-\beta\rangle\langle-\beta|$. As $\beta \rightarrow \infty$, each of these states gives a definite outcome, $+1$ or -1 , respectively, for σ_z^B . This implies that the system B at the initial time is in a state with a predetermined value λ_z^B for the outcome of σ_z^B and S_z^B . Any operations by the superobserver in lab A are local. The system prepared in $\rho_{\text{mix},B}$ remains in a state with the definite value λ_z^B for σ_z^B , throughout the dynamics. The dynamics for the system prepared in $|\psi_{zz}\rangle$ under the evolution U_y^A is *indistinguishable* from that for $\rho_{\text{mix},B}$. That dynamics is therefore consistent with wMR. ■

Result 6.B (2). The dynamics for the superposition $|\psi_{zz}\rangle$ and the mixed state $\rho_{\text{mix},B}$ can diverge, if there are further rotations U_y^A and U_y^B , at both sites.

Proof. This is easy to show, on expansion. We also prove this by example below.

1. Dynamics of the change of measurement setting

We illustrate Result 6.B by examining the dynamics of the measurements. To measure S_y , the superobserver must first reverse the coupling of the system to the friend and meter. The superobserver then performs a local unitary rotation U_y , to change the measurement setting from x to y . This occurs over the timescale associated with U_y . Following that, a pointer measurement occurs by coupling to a second meter in the superobserver's lab, thereby completing the measurement of S_y . We focus on the unitary dynamics U_y , and assume the decoupling from the friend meter has been performed by the time t_2 (Figs. 8 and 7). As outlined in Sec. III, we assume that the reversal takes place at both labs, even where one superobserver may opt to measure S_z .

We first examine $\langle S_y^A S_z^B \rangle$. Here, the superobserver A would apply the unitary rotation $U_A^{-1}(t_a)$ given according to (27). The dynamics to create the state $|\psi_{yz}\rangle_{FR}$ is given by $U_A^{-1}(t_a)|\psi_{zz}\rangle_{FR}$, where $t_a = 3\pi/2\Omega$ so that $U_A^{-1}(t_a) = U_y^A$.

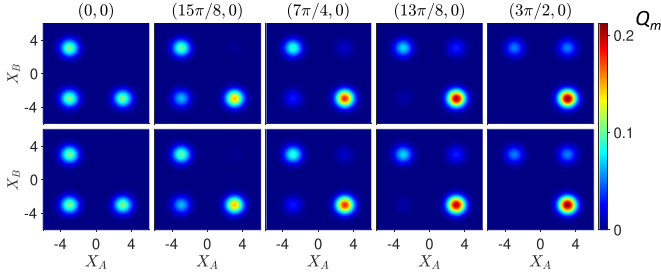


FIG. 10. Dynamics for the single unitary rotation U_y^A associated with the joint measurements of S_y^A and S_z^B by the superobservers is indistinguishable from that of $\rho_{\text{mix},B}$, of Eq. (82). The notation is as for Fig. 9. $\Omega = 1$, $\alpha = 4$. Top sequence: The system begins in $|\psi_{zz}\rangle_{FR}$ [Eq. (38)], and evolves according to U_A^{-1} to the state $|\psi_{yz}\rangle_{FR}$ [Eq. (42)] (far right snapshot). Lower sequence: The system begins in $\rho_{\text{mix},B}$ and evolves as for the top plots. The top and lower sequences are identical, which indicates consistency with weak macroscopic realism (refer to text).

The evolution is pictured as the top sequence of snapshots of Fig. 10. After an interaction time $t_a = -\pi/2\Omega \equiv 3\pi/2\Omega$, the state is $|\psi_{yz}\rangle_{FR}$, for which the Q function is

$$Q_{yz} = \frac{e^{-|\alpha|^2 - X_A^2 - P_A^2 - |\beta|^2 - X_B^2 - P_B^2}}{6\pi^2} \left\{ 4e^{2[\alpha X_A - \beta X_B]} + 4 \cos(2[\alpha P_A - \beta P_B]) - 4e^{2\alpha X_A} \sin(2\beta P_B) + 2e^{2\beta X_B} \cosh(2\alpha X_A) - 2e^{2\beta X_B} \sin(2\alpha P_A) \right\}. \quad (79)$$

The marginal function is

$$Q_{yz}(X_A, X_B) = \frac{e^{-|\alpha|^2 - X_A^2 - |\beta|^2 - X_B^2}}{3\pi} \left\{ 2e^{2[\alpha X_A - \beta X_B]} + 2e^{-\alpha^2 - \beta^2} + e^{2\beta X_B} \cosh(2\alpha X_A) \right\}, \quad (80)$$

as plotted in Fig. 10. Including the treatment of the final coupling to the superobservers' meters M , as above, and then taking γ large, we obtain for the inferred measured amplitudes

$$Q_{yz,mF}(X_A, X_B) = \frac{e^{-|\alpha|^2 - X_A^2 - |\beta|^2 - X_B^2}}{3\pi} \left\{ 2e^{2[\alpha X_A - \beta X_B]} + e^{2\beta X_B} \cosh(2\alpha X_A) \right\}. \quad (81)$$

This agrees with that marginal (80) derived directly from the cat state where $\alpha = \beta$ is large, which is the case of interest.

Similarly, after the appropriate reversal, the measurement S_y at B requires the evolution $U_B^{-1}(t_b)|\psi_{zz}\rangle_{FR}$, which gives after a time $t_b = -\pi/2\Omega \equiv 3\pi/2\Omega$, the state $|\psi_{zy}\rangle_{FR}$. The dynamics for this measurement is plotted in Fig. 11.

After the rotations to measure S_y at both sites, the system is described by $U_A^{-1}U_B^{-1}|\psi_{zz}\rangle_{FR}$, which becomes (for the appropriate interaction times) $|\psi_{yy}\rangle_{FR}$ [Eq. (41)]. The dynamics of these measurements in terms of the Q function is plotted in Fig. 12.

2. Comparison with the classical mixture $\rho_{zz,FR}$: The perspective of the friends

The mixture $\rho_{zz,FR}$ [Eq. (68)] is the state formed from the perspective of the friends, if the two friends have both measured σ_z at their locations e.g., by coupling to the meter. The

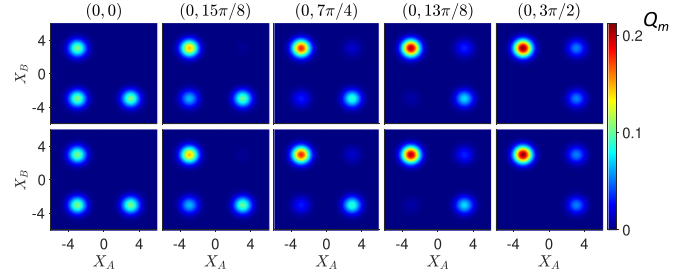


FIG. 11. Dynamics for the single unitary rotation U_y^B associated with the joint measurements of S_z^A and S_y^B by the superobservers is indistinguishable from that of $\rho_{\text{mix},A}$, where friend A 's measurement is not reversed: The notation is as for Fig. 9. Top sequence: The system begins in $|\psi_{zz}\rangle_{FR}$ [Eq. (38)] and evolves according to U_B^{-1} to the state $|\psi_{zy}\rangle_{FR}$ [Eq. (43)] (far right snapshot). Lower sequence: The system begins in $\rho_{\text{mix},A}$ and evolves according to U_B^{-1} as for the top plots. The two sequences are indistinguishable, indicating consistency with weak macroscopic realism (refer to text).

$\rho_{zz,FR}$ describes the statistical state of the system *conditioned* on *both* the friends' outcomes for their measurements of σ_z . The state is conditioned on the outcome $+1$ or -1 for the spins S_z of the meter modes, denoted A_m and B_m in (64), also found by integration of the full Q function over the system and meter variables as explained in Sec. VI A, to derive the result (67). Each meter mode is coupled to the system, so that the systems themselves can continue to evolve, conditioned on the outcome of the measurement on the meter. This evolution is given by that of $\rho_{zz,FR}$.

The dynamics for $\rho_{zz,FR}$ is plotted in Fig. 9, below the dynamics for the superposition state $|\psi_{zz}\rangle_{FR}$. We see that the macroscopic difference between the predictions *emerges over*

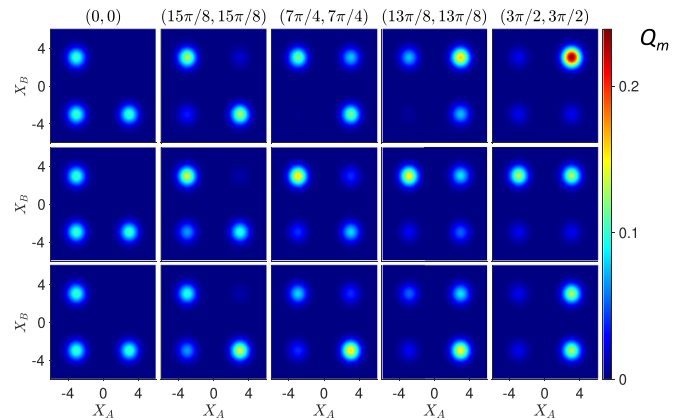


FIG. 12. Dynamics for the two unitary rotations U_y^A and U_y^B associated with the joint measurements of S_y^A and S_y^B by the superobservers. The notation is as for Fig. 9. Top sequence: The system begins in $|\psi_{zz}\rangle_{FR}$ [Eq. (38)] and evolves according to U_A^{-1} and U_B^{-1} to the state $|\psi_{yy}\rangle_{FR}$ [Eq. (41)]. Center (lower) sequence: The system begins in $\rho_{\text{mix},A}$ ($\rho_{\text{mix},B}$) and evolves as for the top plots. The results for $|\psi_{zz}\rangle_{FR}$ diverge macroscopically from those of the mixed states over the dynamics, leading to a violation of the Bell-Wigner inequality for $|\psi_{zz}\rangle_{FR}$. This is not inconsistent with wMR: The wMR premise allows a failure of the macroscopic Bell-locality premise where there are two rotations (refer to Secs. VC and VD2 and Fig. 5).

the timescales of the unitary interaction U_y^A responsible for the change of measurement setting.

The state $\rho_{zz,FR}$ is consistent with a model for which there is a definite predetermined outcome λ_z^A and λ_z^B for σ_z in each lab. The evolution for the system prepared in $\rho_{zz,FR}$ is given as $\rho(t_a, t_b) = U_A^{-1} U_B^{-1} \rho_{zz,FR} U_A U_B$, which satisfies a local realistic theory of the type considered by Bell, and as such does not violate the Bell-Wigner inequality. Hence, the paradox is not realized by $\rho_{zz,FR}$. The superobservers must reverse the friends' measurements in order to restore the state $|\psi_{zz}\rangle_{FR}$. We note the violation of the Bell-Wigner inequality can be inferred, by performing measurements directly on $|\psi_{zz}\rangle_{FR}$, based on the assumption that a measurement of S_z made by the superobservers would yield the same value as that of the friends. It is clear that the predictions and dynamics displayed by the entangled state $|\psi_{zz}\rangle_{FR}$ are not compatible with the mixed state $\rho_{zz,FR}$ [nor any state giving consistency with a local realistic theory, since such a state would not violate (44)].

3. Comparison with partial mixtures: Conditioning on one friend's measurement

We now compare the evolution of $|\psi_{zz}\rangle_{FR}$ with that of partial mixtures obtained by conditioning on the outcomes of one friend. This enables demonstration of the consistency with wMR, using the Result 6.B (1).

First, we consider the dynamics for the measurements of S_z^B and S_y^A , on the system prepared in the state $|\psi_{zz}\rangle_{FR}$. This dynamics creates $|\psi_{yz}\rangle_{FR}$. We compare with the mixture created if the spin measurement σ_z^B made by the friend in L_B is not reversed. The friend has coupled the meter Bm to the system B , as in (64), and conditions all future measurements on the outcome for the meter being +1 or -1. The density operator for the combined system after a measurement of spin σ_z at B is the partial mixture

$$\begin{aligned} \rho_{\text{mix},B} = & \frac{1}{3} |-\alpha\rangle|\beta\rangle\langle\beta|\langle-\alpha| \\ & + \frac{1}{3} (|\alpha\rangle + i|-\alpha\rangle)\langle-\beta|\langle-\beta|(\langle\alpha| - i\langle-\alpha|). \end{aligned} \quad (82)$$

Here, we recall our notation where the first ket we drop the subscripts. Now we consider that a measurement S_y^A is made on system A . This implies (after the appropriate reversal) the evolution according to $U_A^{-1}(t_a)$, which is given in Fig. 10 for both $|\psi_{zz}\rangle_{FR}$ and $\rho_{\text{mix},B}$. Consistent with the predictions of wMR, the evolution of $\rho_{\text{mix},B}$ is indistinguishable from that of $|\psi_{zz}\rangle_{FR}$.

We next consider the dynamics associated with the measurements of S_z^A and S_y^B on the system prepared in $|\psi_{zz}\rangle_{FR}$, which creates $|\psi_{zy}\rangle_{FR}$. For comparison, we also consider that the friend at lab A performs the measurement σ_z^A . The conditioning on the outcomes for the friend's measurement leaves the systems in the mixture

$$\begin{aligned} \rho_{\text{mix},A} = & \frac{1}{3} |\alpha\rangle|-\beta\rangle\langle-\beta|\langle\alpha| \\ & + \frac{1}{3} |-\alpha\rangle(|\beta\rangle + i|-\beta\rangle)\langle\beta| - i_B\langle-\beta|\langle-\alpha|. \end{aligned} \quad (83)$$

The dynamics associated with the measurement of S_y^B involves the system evolving according to $U_B^{-1}(t_b)$, as given in Fig. 11. We see that as consistent with wMR, this evolution for sys-

tems prepared in $|\psi_{zz}\rangle_{FR}$ is indistinguishable from that of systems prepared in $\rho_{\text{mix},A}$.

Finally, we consider the dynamics where measurements of S_y^A and S_y^B are made on the system prepared in the state $|\psi_{zz}\rangle_{FR}$. Here, two local unitary rotations $U_A^{-1}(t_a)$ and $U_B^{-1}(t_b)$ are applied, to create the state $|\psi_{yy}\rangle_{FR}$, prepared in measurement bases for final pointer measurements of S_y^A and S_y^B . We compare this evolution with that of the system prepared in $\rho_{\text{mix},A}$, or $\rho_{\text{mix},B}$ (Fig. 12). The evolution is *macroscopically different* in each case, consistent with the predictions of weak macroscopic realism.

4. Consistency with the weak macroscopic realism model

The predictions of quantum mechanics as given in Figs. 10–12 reveal consistency with weak macroscopic realism (wMR). First, consider measurement of $\langle S_y^A S_z^B \rangle$. The evolution of $|\psi_{zz}\rangle_{FR}$ shown in Fig. 10 is indistinguishable from that of $\rho_{\text{mix},B}$. Hence, from Result 6.B.1, those results show consistency with wMR. After the interaction U_A^{-1} in lab A , the system is prepared in the appropriate basis, so that the final pointer measurement S_y^A can be made by the superobserver. Hence, by Result 6.A, this state is also consistent with wMR. Similarly, prior to the dynamics U_A^{-1} portrayed in the Fig. 10, the superobservers perform the reversal of the friends' measurements. This does not change the preparation basis and, as argued in Sec. VI A, a wMR model exists in which the pointer value $\lambda_z^{B,S} = \lambda_z^B$ is unchanged. We therefore conclude consistency with wMR.

The same arguments apply to the measurement of $\langle S_z^A S_y^B \rangle$. The evolution of $|\psi_{zz}\rangle_{FR}$ shown in Fig. 11 is indistinguishable from that of $\rho_{\text{mix},A}$. Hence, from Result 6.B.1, those results show consistency with wMR.

We have argued that particular models (based on the mixed states) exist that replicate the quantum predictions of the $|\psi_{zz}\rangle_{FR}$, for the moments $\langle S_z^A S_z^B \rangle$, $\langle S_z^A S_y^B \rangle$, and $\langle S_y^A S_z^B \rangle$. At first glance these models seem not consistent, since for the different moments, we consider different mixed states ($\rho_{zz,FR}$, $\rho_{\text{mix},A}$, and $\rho_{\text{mix},B}$) which are not entirely compatible. In fact, we propose a more complete wMR model which includes local operations made by the superobservers. In the model, the system begins in $\rho_{zz,FR}$ at the time t_2 , and consistent with that mixed state, the results for both friends' measurements of σ_z can be known to the superobservers. Where the superobserver A measures S_y by applying U_A^{-1} , then in the model the superobserver A first operates locally in lab A so that the overall system in $\rho_{zz,FR}$ is transformed into $\rho_{\text{mix},B}$. This local operation does not change the value of λ_z^B in the model. Similarly, if superobserver B measures S_y , then in the wMR model, a local operation is performed to change $\rho_{zz,FR}$ into $\rho_{\text{mix},A}$. For this model, wMR holds throughout the dynamics.

In summary, we have shown consistency of the quantum predictions of the Wigner friends paradoxes with both the wMR assertions. This was done using a particular wMR model, and showing compatibility with the predictions for $\langle S_z^A S_z^B \rangle$, $\langle S_z^A S_y^B \rangle$, and $\langle S_y^A S_z^B \rangle$. However, the particular wMR model used is a Bell-local realistic one and does not describe the quantum dynamics for the measurements of S_y at both labs, i.e., where there are two rotations U_y , one at A and one at B . We see from Sec. V however that this does not imply

the quantum predictions are inconsistent with the premise of wMR. The two assertions of wMR are not applicable where there are unitary rotations at *both* sites (refer to Figs. 4, 5, and 12), since both systems shift to a new measurement basis, so that the former pointer values λ^A and λ^B need no longer apply.

VII. CONCLUSION AND DISCUSSION

The motivation of this paper is to present a mapping between the microscopic Wigner's friend paradoxes involving spin qubits and macroscopic versions involving macroscopically distinct "spin" states. In Sec. III, we provide such a mapping, where the macroscopically distinct states are two coherent states, $|\alpha\rangle$ and $|\!-\alpha\rangle$, as $\alpha \rightarrow \infty$. Unitary rotations U determine which spin component is to be measured and in a microscopic spin experiment correspond to Stern-Gerlach analyzers or polarizing beam splitters. In the macroscopic setup, the U are realized with nonlinear interactions.

The mapping motivates us to seek an interpretation for the paradoxes where macroscopic realism can be upheld. The extended Wigner's friend paradoxes are based on plausible assumptions, including that of locality, defined by Bell. We show in Sec. IV that the realizations of the Brukner and Frauchiger-Renner paradoxes each imply falsification of deterministic macroscopic (local) realism.

Motivated by that, we consider in Sec. V a more minimal definition of macroscopic realism, called weak macroscopic realism (wMR), which assigns realism to the system as it exists after the unitary rotation U that determines the measurement setting. This establishes a predetermined value for the outcome of the pointer measurement that is to follow. The premise of wMR also establishes a locality *for this value*: the value is not then affected by events or interactions at a spacelike-separated lab. Careful examination shows that wMR does *not* imply a full locality of the type postulated by Bell, which considers local hidden variables for the system as it exists prior to the unitary dynamics U . In Secs. V–VI, we prove several results which verify that the predictions of quantum mechanics for the paradoxes are consistent with wMR.

A feature of wMR is the definition of realism in a contextual sense. In the wMR model, the state of the system is not defined completely until the measurement basis is specified. The measurement basis for the macroscopic spin system at a given time t is defined as the basis such that the spin can be measured without a further unitary rotation U that would give a change of measurement setting. The final measurement involves a sequence of operations such as amplification and detection, or coupling to meters. These operations are referred to as the final pointer stage of the measurement.

It is possible to define a similar contextual realism for the microscopic qubits. We refer to this as *weak local realism* (wLR). The interpretations of the macroscopic paradoxes can be replicated in the microscopic versions, since there is a mapping between the two. The proofs of the results in Secs. IV–VI follow identically, for the spin-1/2 system. This implies failure of a deterministic local realism, and consistency with weak local realism. Violation of the Bell-CHSH and of Brukner's Bell-Wigner inequality is possible because wLR does *not* imply the full Bell locality assumption.

The results of this paper may give insight into how the assumptions of Bell's theorem break down for quan-

tum mechanics. We find the paradoxes arise only where the measurement setting is changed at *both* sites. This implies two unitary rotations. The unitary dynamics has been analyzed using the Q function. There is an effectively unobservable (as $\alpha \rightarrow \infty$) difference between the Q function of the macroscopic superposition and that of the corresponding mixture (the mixture giving consistency with the Bell-CHSH inequalities). The difference remains undetectable for the case where there is only a single rotation, which gives consistency with a model in which there is a predetermination of one of the measurement outcomes, so that wMR applies. However, where there are two rotations, the Q functions for the states evolving from the macroscopic superposition and the mixture become *macroscopically* different. This leads to macroscopic differences in the predictions, hence allowing the macroscopic paradox to emerge. This is paradoxical, since the final difference between the Q functions is macroscopic in the limit $\alpha \rightarrow \infty$, precisely the limit where the initial difference is increasingly negligible.

While we propose that wMR (and wLR) may hold, we have not presented a full wMR model that replicates all the predictions of quantum mechanics. In particular, we do not propose any specific mechanism for the Bell nonlocality. Arguments have been given elsewhere that there is inconsistency between wMR and the completeness of (standard) quantum mechanics (see, e.g., Refs. [25,30,31]). This motivates examination of alternative theories, or theories which may give a more complete description of quantum mechanics (see, e.g., Refs. [14,34–36,69–78]) for consistency with wMR. It has been shown previously that the Frauchiger-Renner paradox can be explained consistently with Bohm's hidden variable theory, which is highly nonlocal [14]. We leave open the question of whether wMR can be falsified.

Finally, we consider a possible experiment. The microscopic superposition states can be mapped onto coherent-state superpositions using the methods of Refs. [55,56]. The unitary rotations involving Kerr interactions have been realized in experiments creating cat states [41]. The experiments might also be conducted using Greenberger-Horne-Zeilinger states and CNOT gates, as in Ref. [44].

ACKNOWLEDGMENTS

This research has been supported by the Australian Research Council Discovery Project Grants schemes under Grants No. DP180102470 and No. DP190101480. We acknowledge support from the Templeton Foundation under Project Grant ID 62843. The authors wish to thank Nippon Telegraph and Telephone (NTT) Research for their financial and technical support.

APPENDIX

1. Examples of realisation of the friend's cat states

In this paper, we give three examples of a Wigner's friend experiment where the initial spin system is a macroscopic one. The first has been presented in Sec. III. The second example uses GHZ states and CNOT operations. Consider a large number of spin 1/2 qubits. For lab A , we select a set of $N + 1$ qubits, choosing $|h\rangle = |\uparrow\rangle|\uparrow\rangle^{\otimes N}$ and $|t\rangle = |\downarrow\rangle|\downarrow\rangle^{\otimes N}$. Similar macroscopic qubits can be selected for lab B . The

TABLE I. The Table gives along each row a set of possible values that according to deterministic macroscopic realism (dMR) simultaneously predetermine the spin z and spin y outcomes of the bipartite system. All possibilities are given by the 16 rows. The possibilities would not allow a Frauchiger-Renner (FR) paradox to occur. Hence, dMR is falsified by the FR paradox. The full details are explained in Sec. IV B.

λ_{zA}	λ_{zB}	λ_{yA}	λ_{yB}	$P_{-- yy}$	$P_{-+ yy}$	$P_{+- yy}$	$P_{++ yy}$	$P_{-- yz}$	$P_{-- zy}$
1	1	1	1	0	0	0	1	0	0
1	1	1	-1	0	0	1	0	0	0
1	1	-1	1	0	1	0	0	0	0
*1	*1	*-1	*-1	*1	*0	*0	*0	*0	*0
1	-1	1	1	0	0	0	1	0	0
1	-1	1	-1	0	0	1	0	0	0
1	-1	-1	1	0	1	0	0	1	0
1	-1	-1	-1	1	0	0	0	1	0
-1	1	1	1	0	0	0	1	0	0
-1	1	1	-1	0	0	1	0	0	1
-1	1	-1	1	0	1	0	0	0	0
-1	1	-1	-1	1	0	0	0	0	1
-1	-1	1	1	0	0	0	1	0	0
-1	-1	1	-1	0	0	1	0	0	1
-1	-1	-1	1	0	1	0	0	1	0
-1	-1	-1	-1	1	0	0	0	1	1

qubits can be realized as orthogonally polarized photons in $N + 1$ different modes. The coupling to the meters in the labs links the systems to a larger set of M qubits, so that $|H\rangle = |\uparrow\rangle|\uparrow\rangle^{\otimes N}|\uparrow\rangle^{\otimes M}$ and $|T\rangle = |\downarrow\rangle|\downarrow\rangle^{\otimes N}|\downarrow\rangle^{\otimes M}$. The unitary rotation U_x or U_y can be realized using CNOT gates. Suppose the system A is created in $|H\rangle$. Then the photon of the first mode is passed through a beam splitter or polarizing beam splitter, to create

$$(|\uparrow\rangle + e^{i\varphi}|\downarrow\rangle)|\uparrow\rangle^{\otimes(N+M)}. \quad (\text{A1})$$

For each subsequent qubit, a CNOT operation is applied, which creates the Greenberger-Horne-Zeilinger (GHZ) state [45,79–81]

$$|\uparrow\rangle|\uparrow\rangle^{\otimes(N+M)} + e^{i\varphi}|\downarrow\rangle|\downarrow\rangle^{\otimes(N+M)}. \quad (\text{A2})$$

The inclusion of a phase shift φ at the first mode transformation allows either the U_x or the U_y to be realized. Such states have been used to experimentally demonstrate failure of macrorealism [44] and have also been proposed for macroscopic tests of GHZ and Bohm-Einstein-Podolsky-Rosen paradoxes [31], as well as for testing macroscopic Bell inequalities [30].

The third example uses two-mode states and nonlinear interactions. The macroscopic qubits are two-mode number states, given by $|N\rangle_1|0\rangle_2$ and $|0\rangle_1|N\rangle_2$, where $|n\rangle_i$ is a number state for the mode i . These states for large N are

macroscopically distinct. The states were studied in Ref. [38] and [31], where it was shown that a nonlinear interaction H_{nl} (different to (49)) can create the macroscopic cat superposition according to U_x and U_y given by (21) and (22) (where we put $|H\rangle = |N\rangle_1|0\rangle_2$ and $|T\rangle = |0\rangle_1|N\rangle_2$). The transformations are not fully realized, but are sufficiently effective that violation of Bell inequalities are predicted.

2. Meter coupling

Let us consider the qubit $c|\uparrow\rangle + d|\downarrow\rangle$, where c and d are complex amplitudes. We couple the qubit system to a field mode prepared initially in a coherent state $|\gamma_0\rangle$. We consider the evolution under H_{Am} where [82–85]

$$H_{Am} = \hbar G \sigma_z^A \hat{n}_c^A. \quad (\text{A3})$$

Here σ_z^A is the Pauli spin operator for the qubit system A , \hat{n}_c^A is the number operator for the meter mode C in lab A , and G is a real constant. The solution for the final entangled state is

$$\begin{aligned} |\psi\rangle_{\text{out}} &= e^{-iH_{Am}t/\hbar} (c|\uparrow\rangle|\gamma_0\rangle + d|\downarrow\rangle|\gamma_0\rangle) \\ &= c|\uparrow\rangle|\gamma\rangle + d|\downarrow\rangle|-\gamma\rangle, \end{aligned}$$

where we select $Gt = \pi/2$ and $\gamma = -i\gamma_0$.

3. Table of values for macroscopic realistic states

Here, we present the Table I for the proof of Result 4.B of Sec. IV. B. The explanation of the table is given in the main text.

[1] E. P. Wigner, Remarks on the mind-body question, in *Symmetries and Reflections* (Indiana University Press, Bloomington, 1967), pp. 171–184.
[2] C. Brukner, A no-go theorem for observer-independent facts, *Entropy* **20**, 350 (2018).
[3] J. S. Bell, On the Einstein-Podolsky-Rosen paradox, *Physics* (Long Island City, N. Y.) **1**, 195 (1964).

[4] N. Brunner, D. Cavalcanti, S. Pironio, V. Scarani, and S. Wehner, Bell nonlocality, *Rev. Mod. Phys.* **86**, 419 (2014).
[5] J. F. Clauser, M. A. Horne, A. Shimony, and R. A. Holt, Proposed experiment to test local hidden-variable theories, *Phys. Rev. Lett.* **23**, 880 (1969).
[6] J. F. Clauser and A. Shimony, Bell's theorem: Experimental tests and implications, *Rep. Prog. Phys.* **41**, 1881 (1978).

- [7] J. S. Bell, Introduction to the hidden-variable question, in *Foundations of Quantum Mechanics*, edited by B. d'Espagnat (Academic Press, New York, 1971), pp. 171–181.
- [8] D. Frauchiger and R. Renner, Quantum theory cannot consistently describe the use of itself, *Nat. Commun.* **9**, 3711 (2018).
- [9] M. Proietti, A. Pickston, F. Graffitti, P. Barrow, D. Kundys, C. Branciard, M. Ringbauer, and A. Fedrizzi, Experimental test of local observer independence, *Sci. Adv.* **5**, eaaw9832 (2019).
- [10] K.-W. Bong, A. U. Alarcón, F. Ghafari, Y.-C. Liang, N. Tischler, E. G. Cavalcanti, G. J. Pryde, and H. M. Wiseman, A strong no-go theorem on the Wigner's friend paradox, *Nat. Phys.* **16**, 1199 (2020).
- [11] A. Sudbery, Single-world theory of the extended Wigner's friend experiment, *Found. Phys.* **47**, 658 (2017).
- [12] J. Bub, In defense of a single-world interpretation of quantum mechanics, *Stud. Hist. Phil. Mod. Phys.* **72**, 251 (2020).
- [13] R. Healey, Quantum theory and the limits of objectivity, *Found. Phys.* **48**, 1568 (2018).
- [14] D. Lazarovici and M. Hubert, How quantum mechanics can consistently describe the use of itself, *Sci. Rep.* **9**, 470 (2019).
- [15] M. Losada, R. Laura, and O. Lombardi, Frauchiger-Renner argument and quantum histories, *Phys. Rev. A* **100**, 052114 (2019).
- [16] C. Elouard, P. Lewalle, S. K. Manikandan, S. Rogers, A. Frank, and A. N. Jordan, Quantum erasing the memory of Wigner's friend, *Quantum* **5**, 498 (2021).
- [17] A. Matzkin and D. Sokolovski, Wigner friend scenarios with non-invasive weak measurements, *Phys. Rev. A* **102**, 062204 (2020).
- [18] D. Ding, C. Wang, Y.-Q. He, T. Hou, T. Gao, and F.-L. Yan, Tripartite Wigner's friend scenario and its test, *Phys. Scr.* **98**, 075104 (2023).
- [19] M. Lostaglio and J. Bowles, The original Wigner's friend paradox within a realist toy model, *Proc. R. Soc. London, Ser. A* **477**, 20210273 (2021).
- [20] M. Żukowski and M. Markiewicz, Physics and metaphysics of Wigner's friends: Even performed premeasurements have no results, *Phys. Rev. Lett.* **126**, 130402 (2021).
- [21] V. Baumann, F. D. Santo, A. R. H. Smith, F. Giacomini, E. Castro-Ruiz, and C. Brukner, Generalized probability rules from a timeless formulation of Wigner's friend scenarios, *Quantum* **5**, 524 (2021).
- [22] L. Castellani, No relation for Wigner's friend, *Int. J. Theor. Phys.* **60**, 2084 (2021).
- [23] G. Leegwater, When Greenberger, Horne and Zeilinger meet Wigner's friend, *Found. Phys.* **52**, 68 (2022).
- [24] C. Brukner, Wigner's friend and relational objectivity, *Nat. Rev. Phys.* **4**, 628 (2022).
- [25] E. Schrödinger, The present status of quantum mechanics, *Naturwissenschaften* **23**, 823 (1935).
- [26] F. Fröwis, P. Sekatski, W. Dur, N. Gisin, and N. Sangouard, Macroscopic quantum states: Measures, fragility, and implementations, *Rev. Mod. Phys.* **90**, 025004 (2018).
- [27] A. J. Leggett and A. Garg, Quantum mechanics versus macroscopic realism: Is the flux there when nobody looks? *Phys. Rev. Lett.* **54**, 857 (1985).
- [28] C. Emary, N. Lambert, and F. Nori, Leggett–Garg inequalities, *Rep. Prog. Phys.* **77**, 016001 (2014).
- [29] J. S. Bell, in *Foundations of Quantum Mechanics*, edited by B. d'Espagnat (Academic Press, New York, 1971), pp. 171–181.
- [30] M. Thenabadu and M. D. Reid, Bipartite Leggett-Garg and macroscopic Bell inequality violations using cat states: Distinguishing weak and deterministic macroscopic realism, *Phys. Rev. A* **105**, 052207 (2022).
- [31] J. Fulton, R. Y. Teh, and M. D. Reid, preceding paper, Alternative Einstein-Podolsky-Rosen argument based on premises not falsified by Bell's theorem: weak macroscopic realism and weak local realism, *Phys. Rev. A* **110**, 022218 (2024).
- [32] M. Thenabadu and M. D. Reid, Macroscopic delayed-choice and retrocausality: Quantum eraser, Leggett-Garg and dimension witness tests with cat states, *Phys. Rev. A* **105**, 062209 (2022).
- [33] J. Fulton, M. Thenabadu, R.-Y. Teh, and M. D. Reid, Weak versus deterministic macroscopic realism, and Einstein-Podolsky-Rosen elements of reality, *Entropy* **26**, 11 (2024).
- [34] P. Grangier, Contextual inferences, nonlocality, and the incompleteness of quantum mechanics, *Entropy* **23**, 1660 (2021).
- [35] P. D. Drummond and M. D. Reid, Retrocausal model of reality for quantum fields, *Phys. Rev. Res.* **2**, 033266 (2020).
- [36] P. D. Drummond and M. D. Reid, Objective quantum fields, retrocausality and ontology, *Entropy* **23**, 749 (2021).
- [37] B. Yurke and D. Stoler, Generating quantum mechanical superpositions of macroscopically distinguishable states via amplitude dispersion, *Phys. Rev. Lett.* **57**, 13 (1986).
- [38] M. Thenabadu, G.-L. Cheng, T. L. H. Pham, L. V. Drummond, L. Rosales-Zarate, and M. D. Reid, Testing macroscopic local realism using local nonlinear dynamics and time settings, *Phys. Rev. A* **102**, 022202 (2020).
- [39] K. Husimi, Some formal properties of the density matrix, *Proc. Physical Math. Soc. Jpn.* **22**, 264 (1940).
- [40] G. Kirchmair *et al.*, Observation of the quantum state collapse and revival due to a single-photon Kerr effect, *Nature (London)* **495**, 205 (2013).
- [41] B. Vlastakis, G. Kirchmair, Z. Leghtas, S. E. Nigg, L. Frunzio, S. M. Girvin, M. Mirrahimi, M. H. Devoret, and R. J. Schoelkopf, Deterministically encoding quantum information using 100-photon Schrödinger cat states, *Science* **342**, 607 (2013).
- [42] M. Greiner, O. Mandel, T. Hänsch, and I. Bloch, Collapse and revival of the matter wave field of a Bose-Einstein condensate, *Nature (London)* **419**, 51 (2002).
- [43] E. M. Wright, D. F. Walls, and J. C. Garrison, Collapses and revivals of Bose-Einstein condensates formed in small atomic samples, *Phys. Rev. Lett.* **77**, 2158 (1996).
- [44] H.-Y. Ku, N. Lambert, F.-J. Chan, C. Emary, Y.-N. Chen, and F. Nori, Experimental test of non-macrorealistic cat states in the cloud, *npj Quantum Inf.* **6**, 98 (2020).
- [45] A. Omran, H. Levine, A. Keesling, G. Semeghini, T. T. Wang, S. Ebadi, H. Bernien, A. S. Zibrov, H. Pichler, S. Choi *et al.*, Generation and manipulation of Schrödinger cat states in Rydberg atom arrays, *Science* **365**, 570 (2019).
- [46] M. Brune, E. Hagley, J. Dreyer, X. Maitre, A. Maali, C. Wunderlich, J. Raimond, and S. Haroche, Observing the progressive decoherence of the “meter” in a quantum measurement, *Phys. Rev. Lett.* **77**, 4887 (1996).
- [47] C. Monroe, D. M. Meekhof, B. E. King, and D. J. Wineland, A “Schrödinger cat” superposition state of an atom, *Science* **272**, 1131 (1996).

- [48] A. Ourjoumtsev, H. Jeong, R. Tualle-Brouiri, and P. Grangier, Generation of optical Schrödinger cats from photon number states, *Nature (London)* **448**, 784 (2007).
- [49] L. Krippner, W. J. Munro, and M. D. Reid, Transient macroscopic quantum superposition states in degenerate parametric oscillation: Calculations in the large-quantum-noise limit using the positive P representation, *Phys. Rev. A* **50**, 4330 (1994).
- [50] L. Gilles, B. M. Garraway, and P. L. Knight, Generation of nonclassical light by dissipative two-photon processes, *Phys. Rev. A* **49**, 2785 (1994).
- [51] E. E. Hach III and C. C. Gerry, Generation of mixtures of Schrödinger-cat states from a competitive two-photon process, *Phys. Rev. A* **49**, 490 (1994).
- [52] M. Wolinsky and H. J. Carmichael, Quantum noise in the parametric oscillator: From squeezed states to coherent-state superpositions, *Phys. Rev. Lett.* **60**, 1836 (1988).
- [53] R. Y. Teh, F. X. Sun, R. E. S. Polkinghorne, Q. Y. He, Q. Gong, P. D. Drummond, and M. D. Reid, Dynamics of transient cat states in degenerate parametric oscillation with and without nonlinear Kerr interactions, *Phys. Rev. A* **101**, 043807 (2020).
- [54] M. Thenabadu and M. D. Reid, Leggett-Garg tests of macrorealism for dynamical cat states evolving in a nonlinear medium, *Phys. Rev. A* **99**, 032125 (2019).
- [55] Z. Leghtas, G. Kirchmair, B. Vlastakis, M. H. Devoret, R. J. Schoelkopf, and M. Mirrahimi, Deterministic protocol for mapping a qubit to coherent state superpositions in a cavity, *Phys. Rev. A* **87**, 042315 (2013).
- [56] C. Wang *et al.*, A Schrödinger cat living in two boxes, *Science* **352**, 1087 (2016).
- [57] R. Uola, G. Vitagliano and C. Budroni, Leggett-Garg macrorealism and the quantum nondisturbance conditions, *Phys. Rev. A* **100**, 042117 (2019).
- [58] O. J. E. Maroney and C. G. Timpson, Quantum- vs. macrorealism: What does the Leggett-Garg inequality actually test? [arXiv:1412.6139](https://arxiv.org/abs/1412.6139).
- [59] G. C. Knee, K. Kakuyanagi, M.-C. Yeh, Y. Matsuzaki, H. Toida, H. Yamaguchi, S. Saito, A. J. Leggett and W. J. Munro, A strict experimental test of macroscopic realism in a superconducting flux qubit, *Nat. Commun.* **7**, 13253 (2016).
- [60] H. Jeong, M. Paternostro, and T. C. Ralph, Failure of local realism revealed by extremely-coarse-grained measurements, *Phys. Rev. Lett.* **102**, 060403 (2009).
- [61] A. Aspect, P. Grangier, and G. Roger, Experimental realization of Einstein-Podolsky-Rosen-Bohm gedankenexperiment: A new violation of Bell's inequalities, *Phys. Rev. Lett.* **49**, 91 (1982).
- [62] D. Bohm and Y. Aharonov, Discussion of experimental proof for the paradox of Einstein, Rosen, and Podolsky, *Phys. Rev.* **108**, 1070 (1957).
- [63] Y. Aharonov and L. Vaidman, Complete description of a quantum system at a given time, *J. Phys. A: Math. Gen.* **24**, 2315 (1991).
- [64] R. E. George, L. Robledo, O. J. E. Maroney, M. S. Blok, H. Bernien, M. L. Markham *et al.*, Opening up three quantum boxes causes classically undetectable wavefunction collapse, *Proc. Natl. Acad. Sci. USA* **110**, 3777 (2013).
- [65] K. J. Resch, J. S. Lundeen, and A. M. Steinberg, Experimental realization of the quantum box problem, *Phys. Lett. A* **324**, 125 (2004).
- [66] O. J. E. Maroney, Measurements, disturbance and the three-box paradox, *Stud. Hist. Philos. Sci. B*, **58**, 41 (2017).
- [67] C. Hatherasinghe, M. Thenabadu, P. D. Drummond, and M. D. Reid, A macroscopic quantum three-box paradox: Finding consistency with weak macroscopic realism, *Entropy* **25**, 1620 (2023).
- [68] P. Colciaghi, Y. Li, P. Treutlein, and T. Zibold, Einstein-Podolsky-Rosen experiment with two Bose-Einstein condensates, *Phys. Rev. X* **13**, 021031 (2023).
- [69] D. Bohm, A suggested interpretation of quantum theory in terms of hidden variables, *Phys. Rev.* **85**, 166 (1952).
- [70] M. J. W. Hall, D.-A. Deckert, and H. M. Wiseman, Quantum phenomena modeled by interactions between many classical worlds, *Phys. Rev. X* **4**, 041013 (2014).
- [71] H. Price, Toy models for retrocausality, *Stud. Hist. Phil. Mod. Phys.* **39**, 752 (2008).
- [72] S. Donadi and S. Hossenfelder, Toy model for local and deterministic wave-function collapse, *Phys. Rev. A* **106**, 022212 (2022).
- [73] K. B. Wharton and N. Argaman, Colloquium: Bell's theorem and locally mediated reformulations of quantum mechanics, *Rev. Mod. Phys.* **92**, 021002 (2020).
- [74] S. Frederich, Introducing the Q -based interpretation of quantum theory, [arXiv:2106.13502](https://arxiv.org/abs/2106.13502).
- [75] R. B. Griffiths, *Consistent Quantum Theory* (Cambridge University Press, Cambridge, 2002).
- [76] G. Castagnoli, Unobservable causal loops explain both the quantum computational speedup and quantum nonlocality, *Phys. Rev. A* **104**, 032203 (2021).
- [77] R. B. Griffiths, Nonlocality claims are inconsistent with Hilbert-space quantum mechanics, *Phys. Rev. A* **101**, 022117 (2020).
- [78] R. W. Spekkens, Evidence for the epistemic view of quantum states: A toy theory, *Phys. Rev. A* **75**, 032110 (2007).
- [79] D. M. Greenberger, M. A. Horne, and A. Zeilinger, Bell's theorem without inequalities, *Am. J. Phys.* **58**, 1131 (1990).
- [80] N. D. Mermin, Extreme quantum entanglement in a superposition of macroscopically distinct states, *Phys. Rev. Lett.* **65**, 1838 (1990).
- [81] D. M. Greenberger, M. Horne, and A. Zeilinger, Going beyond Bell's theorem, in *Quantum Theory, and Conceptions of the Universe*, edited by M. Kafatos (Kluwer, Dordrecht, 1989), p. 69.
- [82] L. Rosales-Zárate, B. Opanchuk, and M. D. Reid, Weak measurements and quantum weak values for NOON states, *Phys. Rev. A* **97**, 032123 (2018).
- [83] E. O. Ilo-Okeke and T. Byrnes, Theory of single-shot phase contrast imaging in spinor Bose-Einstein condensates, *Phys. Rev. Lett.* **112**, 233602 (2014).
- [84] A. Blais, R.-S. Huang, A. Wallraff, S. M. Girvin, and R. J. Schoelkopf, Cavity quantum electrodynamics for superconducting electrical circuits: An architecture for quantum computation, *Phys. Rev. A* **69**, 062320 (2004).
- [85] A. Wallraff, D. I. Schuster, A. Blais, L. Frunzio, R.-S. Huang, J. Majer, S. Kumar, S. M. Girvin, and R. J. Schoelkopf, Strong coupling of a single photon to a superconducting qubit using circuit quantum electrodynamics, *Nature (London)* **431**, 162 (2004).